Geomorphology 101 (2008) 703–720

Contents lists available at ScienceDirect

Geomorphology

journal homepage: www.elsevier.com/locate/geomorph

Transverse Aeolian Ridges (TARs) on Mars

Matt Balme [a,b,*], Daniel C. Berman [a], Mary C. Bourke [a], James R. Zimbelman [c]

[a] Planetary Science Institute, 1700 E. Fort Lowell, Suite 106, Tucson, AZ 85719, USA
[b] Department of Earth Sciences, The Open University, Walton Hall, Milton Keynes, England, MK7 6AA, United Kingdom
[c] Center for Earth and Planetary Studies, National Air and Space Museum, Smithsonian Institution, PO Box 37012, National Air and Space Museum, MRC 315, Washington, DC 20013-7012, USA

ARTICLE INFO

Article history:
Received 31 July 2007
Received in revised form 26 March 2008
Accepted 26 March 2008
Available online 9 April 2008

Keywords:
Mars
Ripples
Dunes
Aeolian
Planetary geomorphology

ABSTRACT

Aeolian processes are probably the dominant ongoing surface process on Mars; Large Dark Dunes (LDDs), particularly common aeolian landforms, were first recognized in the early 1970s. Recent, higher resolution images have revealed another, morphologically distinct, large population of smaller, ripple-like aeolian bedforms that have been termed "Transverse Aeolian Ridges" (TARs) as it is unknown whether they formed as large ripples or small dunes. We have begun a new study of TARs that examines their distribution, orientation, and morphology using >10,000 high-resolution Mars Orbiter Camera (1.5 to 8 m/pixel resolution) images in a 45° longitude wide, pole-to-pole survey. The aim of this study is to assess whether TARs are active, to identify possible sediment sources and pathways, and to determine the volumes of sediment that they comprise. We present results from the first half of this study, in which we examine the northern hemisphere, and describe a new three-part classification scheme used to aid the survey.

Our results show that TARs are abundant but not ubiquitous: preferentially forming proximal to friable, layered terrains such as those found in Terra Meridiani — the location of the ongoing Mars Exploration Rover "Opportunity" mission. TAR distribution in the northern hemisphere shows a strong latitudinal dependence with very few TARs being found north of ~30° N. We also find that in most cases TARs are less mobile than LDDs, a conclusion possibly explained by Mars Exploration Rover Opportunity observations that show TAR-like ripples to have a core of fine material armored by a monolayer of granule-sized particles. This could disallow significant bedform movement under the current wind regime. That TARs are essentially inactive is confirmed by superposition relations with slope streaks and LDDs and by observations of superposed impact craters. We suggest that observations made by the Opportunity Rover in Terra Meridiani indicate that the small aeolian bedforms common here are ripples and not small dunes. Farther south, these bedforms transition into larger features indistinguishable from TARs, suggesting that TARs (in the Meridiani area at least) are ripples and not dunes.

1. Introduction

Mars currently has an atmosphere about two orders of magnitude thinner than the Earth's and yet hosts a range of aeolian landforms similar to those of our own planet. Examples of dunes, ripples, dust devils, dust storms, yardangs, and ventifacts can all be found on Mars and demonstrate coupling between the atmosphere and the surface over a range of temporal and spatial scales. Dunes were first identified on Mars from Mariner 9 images (McCauley et al., 1972; Cutts and Smith, 1973). Later, Mariner and Viking orbiter images revealed a series of extensive ergs around the north pole ice cap (Cutts et al., 1976; Tsoar et al., 1979) and large dune fields in craters in the southern hemisphere (Cutts and Smith, 1973; Thomas, 1981; Lancaster and Greeley, 1987). The defining features of both the northern and southern dune fields are the low albedo and large size of the duneforms. Where dunes are coalesced, crest to crest wavelengths are typically hundreds to a few thousands of meters (Greeley et al., 1992; Fig. 1a and b).

However, as noted first from Viking images (Zimbelman, 1987) and more recently from Mars Global Surveyor (MGS) Mars Orbiter Camera (MOC) narrow angle (NA) images (Thomas et al., 1999; Malin and Edgett, 2001), another morphologically and dimensionally distinct population of aeolian bedforms exists that are generally brighter than, or of similar albedo to, the surrounding terrain (Malin and Edgett, 2001; Fig. 1c and d). These features are smaller than the dark dunes, being of decameter scale and appear to form normal to local winds. They tend to have simple, transverse, 'ripple-like' morphologies leading several authors (e.g., Williams et al., 2002; Zimbelman and Wilson, 2002; Wilson et al., 2003) to suggest that these bedforms might be analogous to large terrestrial ripples termed "aeolian ridges" (Bagnold, 1941), 'granule ripples' (Sharp, 1963; Fryberger et al., 1992) or 'mega-ripples' (Greeley and Iversen, 1985). However, whether these

* Corresponding author. Planetary Science Institute, 1700 E. Fort Lowell, Suite 106, Tucson, AZ 85719, USA.
E-mail address: mbalme@psi.edu (M. Balme).

0169-555X/$ – see front matter © 2008 Elsevier B.V. All rights reserved.
doi:10.1016/j.geomorph.2008.03.011

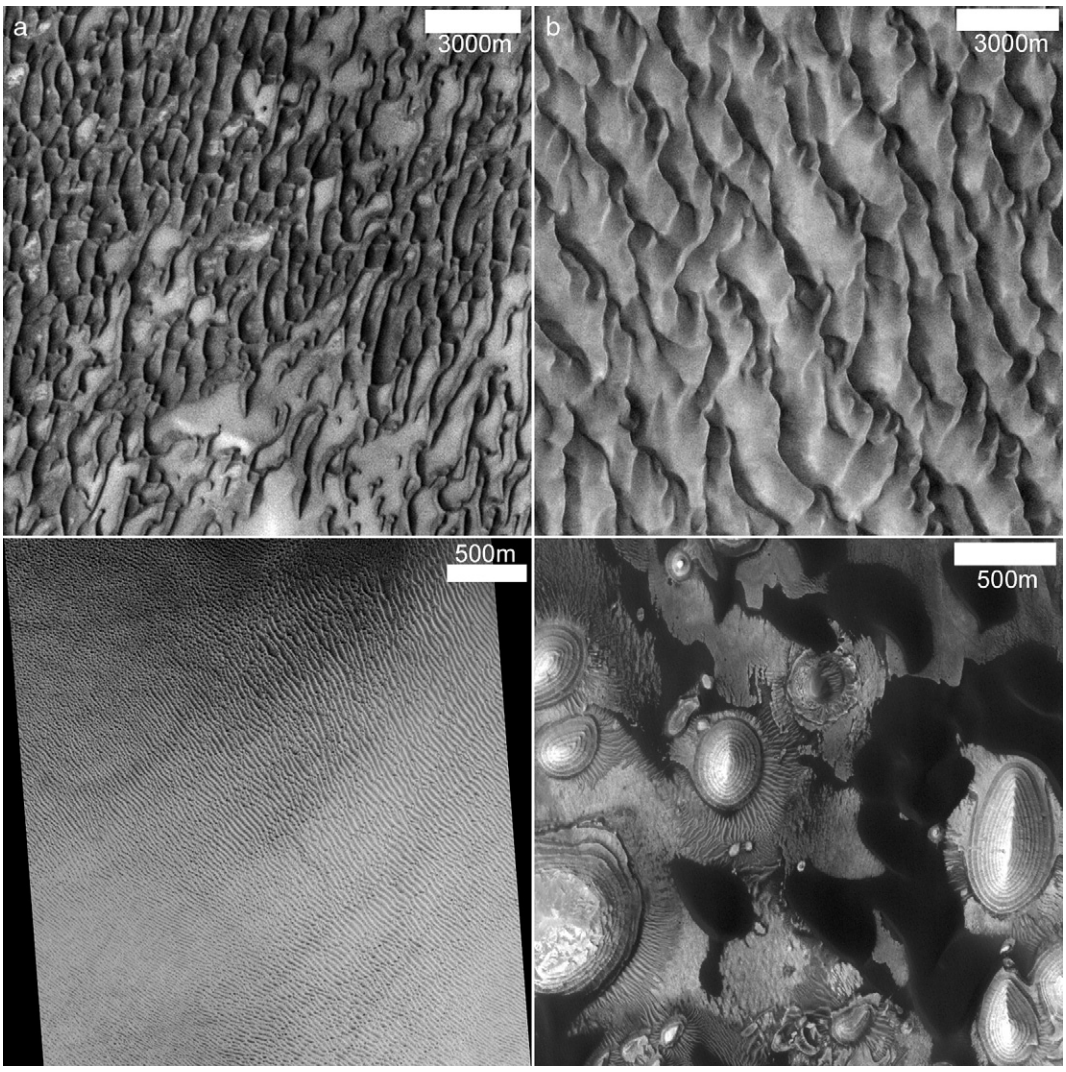

Fig. 1. Examples of TARs compared with LDDs. Note the difference in scale between the images. (a) LDDs in the north polar sand sea. THEMIS visible image V04495014. (b) LDDs from the southern highlands Proctor Crater dune field. THEMIS visible image V15926001. (c) Extensive TARs in a crater at ~47.5 S. 37 E. MOC NA image R0902119. (d) TARs and LDDs, together with spectacular layered mesas at ~8.8 N. 358.5 E. MOC NA image S0700608. North is up in this and all other remote sensing figures except where noted. Image credits NASA/JPL/ASU/MSSS.

small martian bedforms represent extremely large ripples or small transverse dunes is currently unknown, and so they have been called "Transverse Aeolian Ridges" (TARs) by Bourke et al. (2003) in remote sensing studies, a label with little genetic inference. The question of whether TARs are dunes or ripples is discussed further in Section 5.1.

TARs are found in almost all settings, from the highest volcanoes (Malin and Edgett, 2001) to the floor of the deepest impact basins (a nearly 30 km elevation range); but their sediment source, age, superposition relationships, and degree of migration activity are largely unknown. This paper is part of a larger project to survey high-resolution images in a pole-to-pole swath between 0 to 45° E. longitude to determine some of these unknowns, and also reports the results of a smaller survey in the Terra Meridiani region of Mars. Here we summarize previous work, present new observations of TARs, describe a new classification scheme, and present preliminary results from the pole-to-pole survey. In many situations, we compare and contrast the behavior of TARs with the other common aeolian bedform type on Mars: the Large Dark Dunes (LDDs). Our aim is to investigate if TARs and LDDs form contemporaneously or require different climatic conditions, whether TARs and LDDs are composed of similar sediment (composition and texture), and to estimate how active TARs are compared to LDDs.

2. Approach

In contrast to Earth remote sensing studies, *in situ* observations of landforms observed in spacecraft images are rare for Mars (only five extremely small areas have been observed from the surface, those at the Viking 1 and 2, Mars Pathfinder and the two Mars Exploration Rover landing sites) so there is little scope for ground truth. A robust identification strategy for landforms studied only by remote sensing is therefore important. We have used MOC NA data almost exclusively in this study, these being a high-resolution, grayscale imaging product with >210,000 images publicly available and a surface coverage >7%. At MOC NA resolution (sometimes ~1 m/pixel but more frequently 1.5–12 m/pixel), identification of TARs is usually straightforward as they have distinctive ripple-like morphologies with no obvious slip face and generally form in accumulations of a few to thousands of bedforms.

However some morphologies occur that are more difficult to interpret and some terrains exist that might easily be mistaken for TARs, especially in cases where the image is noisy or has poor spatial or radiometric resolution. In particular, mid-latitude deposits associated with fretted terrain (kilometer-scale mesas and buttes forming an eroded margin between the cratered southern highlands and the northern lowland plains), lobate debris aprons, and lineated valley fill

materials, thought to be of glacial origin (Mangold, 2003; Pierce and Crown, 2003), are often similar in appearance to TARs (Fig. 2a). Morphological observations that suggest these features are not TARs include the lack of a defined crest ridge, superposition and alteration of pre-existing topography, and burial or exhumation from under a smoother layer (although this does not preclude them being relict aeolian bedforms). In addition, examining MOC wide angle (WA) images for context often reveals that these terrains are associated with debris aprons around mesas, at the bases of scarps, or within valleys; and they frequently have orientation trends normal to the local slope. Taken together with the morphological observations, these associations suggest that they are not aeolian landforms. Other morphologies that are difficult to discern from TARs include network ridge patterns (Fig. 2b) found in certain debris aprons and morphologically similar to the "sharp ridge" textures described by Pierce and Crown (2003), polygonal terrains similar to networked TARs (Fig. 2c), and lineated terrain (Fig. 2d) found occasionally in the north and south mid to high polar regions. These examples might represent the products of weathered or eroded aeolian bedforms, periglacial processes, or exhumed terrains (e.g., Mangold, 2005).

For the pole-to-pole survey, we first generated a list of MOC NA images within the study area from the NASA PDS website (http://pds-imaging.jpl.nasa.gov/Missions/MGS_mission.html). The list includes all images up to the January 2006 data release. Corrupt, noisy, or low resolution images (poorer than 10 m/pixel) were excluded. Each image was searched for TARs at full resolution, erring on the side of caution to exclude examples with morphologies/associations described above. The percentile areal coverage of TARs was recorded for each image studied as well as a classification of TARs (see Section 3.2 below), associations with other landforms, and general observations. Finally, those images with >5% TAR coverage were reprocessed and map-projected using USGS ISIS software and imported into Geographical Information Systems software for analysis.

3. Remote sensing observations of TARs

3.1. Physical description

TARs typically form in small fields of tens to thousands of individual bedforms and are characterized by their small size, narrow transverse dimensions, and elongate and generally simple form. Slip faces are typically not resolvable in MOC NA images, and lee and stoss slopes appear to be approximately symmetric (Malin and Edgett, 2001; Bourke et al., 2006).

TARs can be described by three principal morphometric parameters: the crest-ridge width *W*, the "down wind" TAR length *L*, and

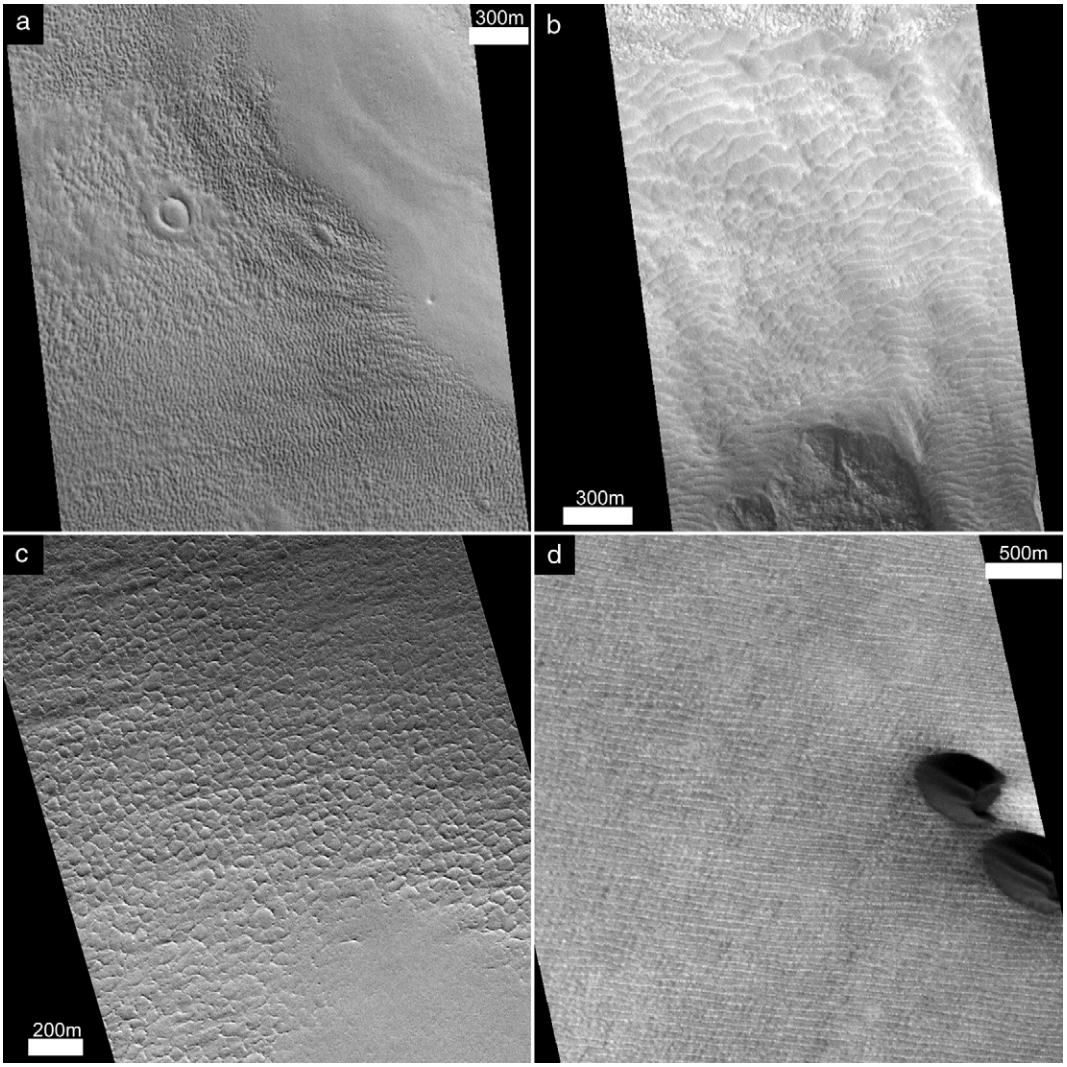

Fig. 2. Examples of morphologies that might be confused with TARs. (a) Fretted debris apron at ~45.9 N. 44.8 E. MOC NA image M0802614. (b) Sharp ridge terrain in fretted debris apron at ~43.8 N. 35.6 E. MOC NA image M0706084. (c) North polar polygonal terrain. MOC NA image E2000607. (d) North polar lineated terrain. MOC NA image E2300658. Image credits NASA/JPL/MSSS.

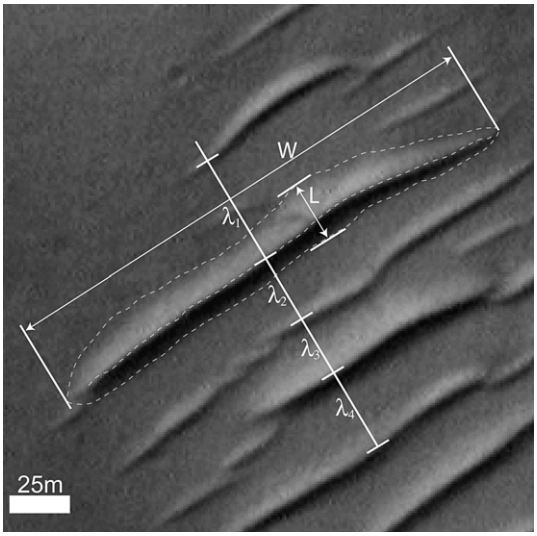

Fig. 3. Example of morphometric parameters used to describe TARs. The mean profile λ is given by the average of λ_{1-4} MOC NA image E2100624. Image credit NASA/JPL/MSSS.

the ridge-to-ridge spacing λ (where λ is the mean spacing calculated as shown in shown in Fig. 3). In addition, from these basic measurements we define plan view aspect ratio *a*, where $a = W / L$, and inter-bedform spacing *s*, where $s = \lambda / L$. Wilson and Zimbelman (2004) measured physical dimensions of >340 TARs from 172 MOC NA images and found a mean wavelength of ~40 m, with a typical range of 10–60 m. The mean crest length was 215 m, with a standard deviation of 155 m. Wilson and Zimbelman (2004) found no unambiguous correlation between wavelength and crest length, but Bourke et al. (2003) did find that TARs seem to be more closely-spaced in the narrowest parts of troughs and valleys. TARs generally have high plan view aspect ratios, typically >6 and sometimes up to 15 (Thomas et al., 1999), although many examples of bedforms with low plan view aspect ratio exist that we also classify as TARs (Fig. 4). Plan view aspect ratio and inter-bedform spacing can be easily estimated in qualitative terms. For example, closely-spaced TARs with $s = 1$ or <2 are easily distinguished from widely spaced TARs with $s > \sim 5$ (Fig. 5). In general we refer to deposits of TARs with $s = 1$ as "saturated", $s < 2$ as being "closely-spaced", and those with higher *s* values as being "discontinuous" or "widely spaced".

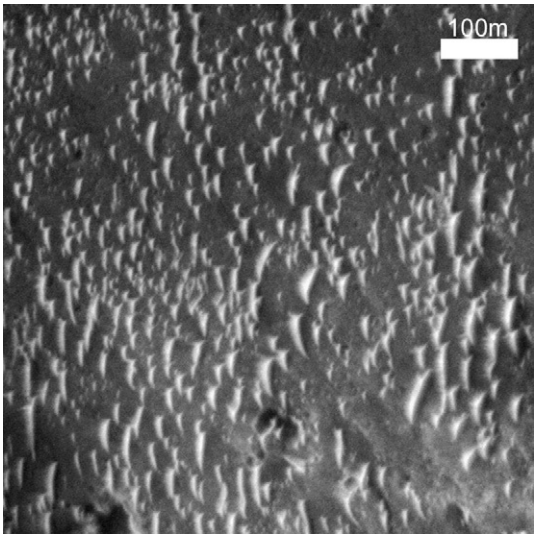

Fig. 4. Blunt TARs in north Sinus Meridiani with lower crest-ridge width to bedform length ratios than are found in the majority of TARs. Many of these TARs have plan view aspect ratios of only 2 or 3. MOC NA image R1201434. Image credit NASA/JPL/MSSS.

Ridge heights are difficult to obtain because of the lack of *in situ*, high-resolution stereo or reliable photoclinometry data, although this situation is improving with new images from missions such as Mars

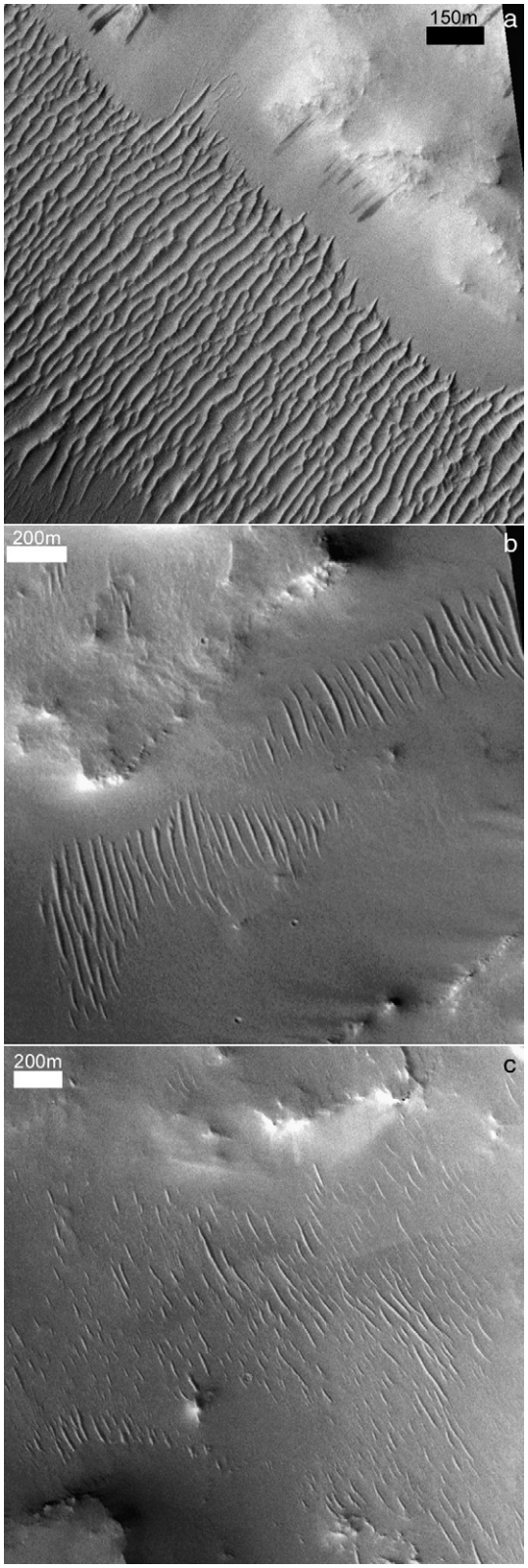

Fig. 5. Examples of variation in TAR inter-bedform spacing. (a) Saturated TARs with $s \sim 1$ at ~0.1 N., 37.8 E. MOC NA image R0400111. (b) TARs with a medium inter-bedform spacing (*s* is ~2 to 3 for most of these TARs) at ~24 N., 34.3 E. MOC NA image M0705509 (c) unsaturated or widely spaced TARs ($s > 5$ for most of these TARs) at ~19.5 N., 35.3 E. MOC NA image M0900169. Image credit NASA/JPL/MSSS.

Reconnaissance Orbiter (MRO), currently in Mars orbit. Some estimates have been made using methods such as low sun-angle measurements of shadow length (TAR height <1.5 m; Zimbelman, 2000); stereo imaging from overlapping MOC NA images (TAR height ~5.7 m; Williams et al., 2003); photoclinometry, slip face measurements, and stereography (TAR heights 1–7.8 m; Bourke et al., 2006), and extrapolation from terrestrial examples, (TAR heights 1–3 m for a 40 m wavelength TAR; Wilson et al., 2003). Few data exist that allow systematic comparisons of ripple index (height/wavelength) for TARs on Mars with the value of ~1/15 given by Sharp (1963) for ripples on Earth, although Zimbelman and Williams (2007) have begun the process using photometric methods and new MRO High Resolution Imaging Science Experiment (HiRISE) data. They obtained a transverse height profile of a TAR and compared this with similar data for terrestrial granule ripples and transverse dunes, finding that the TAR was most similar in profile shape to the terrestrial granule ripple but much taller with respect to its wavelength (Fig. 6). The TAR was dissimilar in profile shape to the transverse dunes they studied and also had a much higher height/wavelength ratio; transverse dunes on Earth in general have lower height/wavelength ratios (1/20 to 1/30; Lancaster, 1995) than ripples or granule ripples.

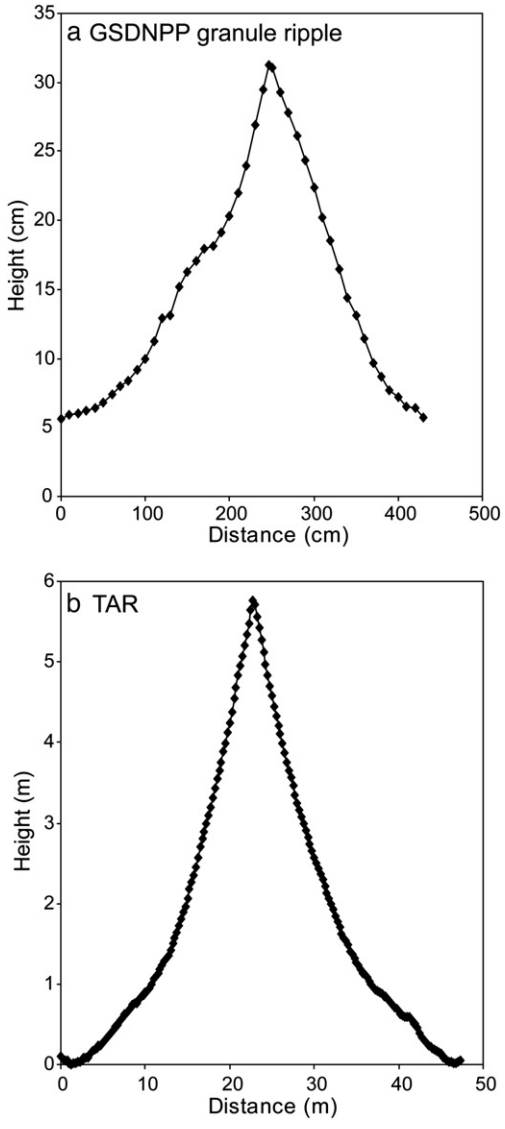

Fig. 6. Profiles across a large granule ripple in the Great Sand Dunes National Park and Preserve (a) and a TAR on Mars (b). The wind is from the right in (a) and is unknown in (b). The ripple index is ~1/15 for the granule ripple and 1/8 for the TAR. After Zimbelman et al. (2007).

3.2. Classification of TAR deposits

TARs have been classified previously by Bourke et al. (2003) and Wilson and Zimbelman (2004). Bourke et al. used plan view shape of the bedform crest ridges as the basis of their classification scheme but limited their study to TARs within troughs. Wilson and Zimbelman based their classification scheme on a combination of shape, associations, and level of topographic control of the TARs in a deposit. Building on the classifications of these authors and our own preliminary global study of several hundred MOC NA images, we present a new three-level scheme that describes TAR deposits in terms of the morphology of the crest ridges, the degree of topographic control of the deposit, and the total size (or number of bedforms) of the deposit.

The aim of the classification scheme is to assist geographic analysis of TAR distribution and evolution. Using the three-part scheme, we can identify spatial variations in types of TARs, find areas where regional, rather than local, wind regimes shape TARs, and identify those areas with the largest TAR deposits.

3.2.1. Crest-ridge morphology

In this study, we have noted five first-order crest-ridge plan view morphologies: “simple”, “sinuous”, “forked”, “networked”, and “barchan-like”. Examples of these classifications are shown in Fig. 7. Unlike Bourke et al. (2003), ‘feathered TARs’ are not considered to be a first-order classification here, but instead this morphology is suggested to represent secondary crests superposed upon the primary bedforms, as discussed in Section 3.6. Sometimes these five morphologies can exist within the same TAR deposit: we discuss in Section 3.6 whether these morphologies represent evolutionary stages, are tied to sediment supply, or are a function of wind regime.

3.2.2. Degree of topographic control

The orientation of TARs can indicate whether local topography or regional meteorology controls the evolution of the TAR accumulation. In contrast to the Earth where we can study aeolian deposits *in situ*, on Mars we must rely on secondary evidence to provide clues as to whether they are active or inactive, or if the deposit represents a depositional or transportational environment. We have therefore developed a classification scheme for the degree of topographic control of TARs. The scheme considers the situation of the TARs with respect to local topographic obstructions, whether positive or negative relief, and their effect on the ridge-crest orientations of the TARs. We have identified four topographic environments: (i) “Confined”: the TAR deposit is located within a closed topographic basin or depression. Crest-ridge orientations and spacing are commonly controlled by the boundaries of the depression, reflecting deflection and modulation of the regional wind by local topography. Where adjacent TAR deposits exist, crest-ridge orientations can therefore be dissimilar. Impact craters are common environments for confined TARs (Fig. 8a). (ii) “Controlled”: the TARs are located within a depression or valley or adjacent to a local topographic high. An important difference from the confined class is that the depression is open. Again, the orientation and spacing of the TARs are dominated by the boundary conditions and reflect local-scale deflections of wind by topography. Common environments for controlled TARs include the floors of valleys and troughs and adjacent to the bases of scarps and cliffs (Fig. 8b). (iii) “Influenced”: the overall distribution of the TARs is not dominated by the terrain, although on a small scale the orientations of individual TARs are clearly influenced by topography. Examples include TARs deflected by small mesas or hills and TARs that formed over and around small impact craters (Fig. 8c). (iv) “Independent”: the orientation of TARs is consistent over a large area and not influenced by local topography. Such environments include very flat or gently sloping topography, regions where topographic variations are very minor, or any area where regional wind regime dominated the effects of local topography (Fig. 8d).

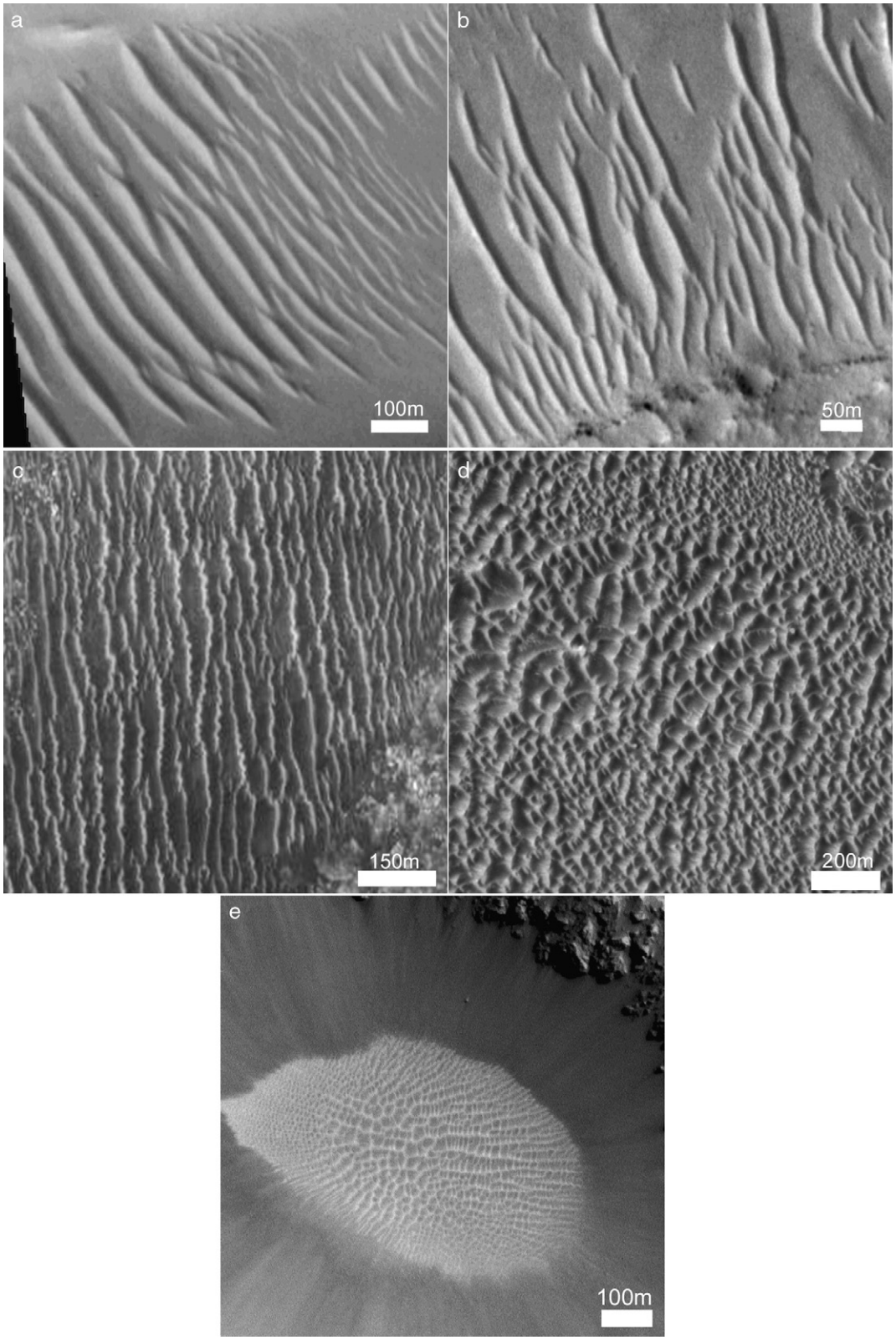

Fig. 7. Examples of each of the five TAR crest-ridge morphologies. (a) Simple, at ~21.3 N., 39.3 E. MOC NA image M1104208. (b) Forked, at ~20.7 N., 41.3 E. MOC NA image M0303703. (c) Sinuous, at ~45.5 S., 28.7 E. MOC NA image R0802177. (d) Barchan-like, at ~0.2 N., 0.1 E. MOC NA image M1800277. (e) Networked, at ~0.1 S., 5.3 E. MOC NA image R2300801. Image credits NASA/JPL/MSSS.

3.2.3. Size of TAR accumulation

A spatially continuous TAR deposit can be many square kilometers in extent and comprise hundreds or thousands of bedforms or can consist of only a few individual TARs and cover an area less than a few 100 m^2. Being able to describe a TAR deposit in simple terms to give an indication of the volumes of sediment involved and/or the spatial extent of the deposit is therefore useful. Several challenges to developing a classification of TAR deposits by size exist: (i) TARs within large deposits

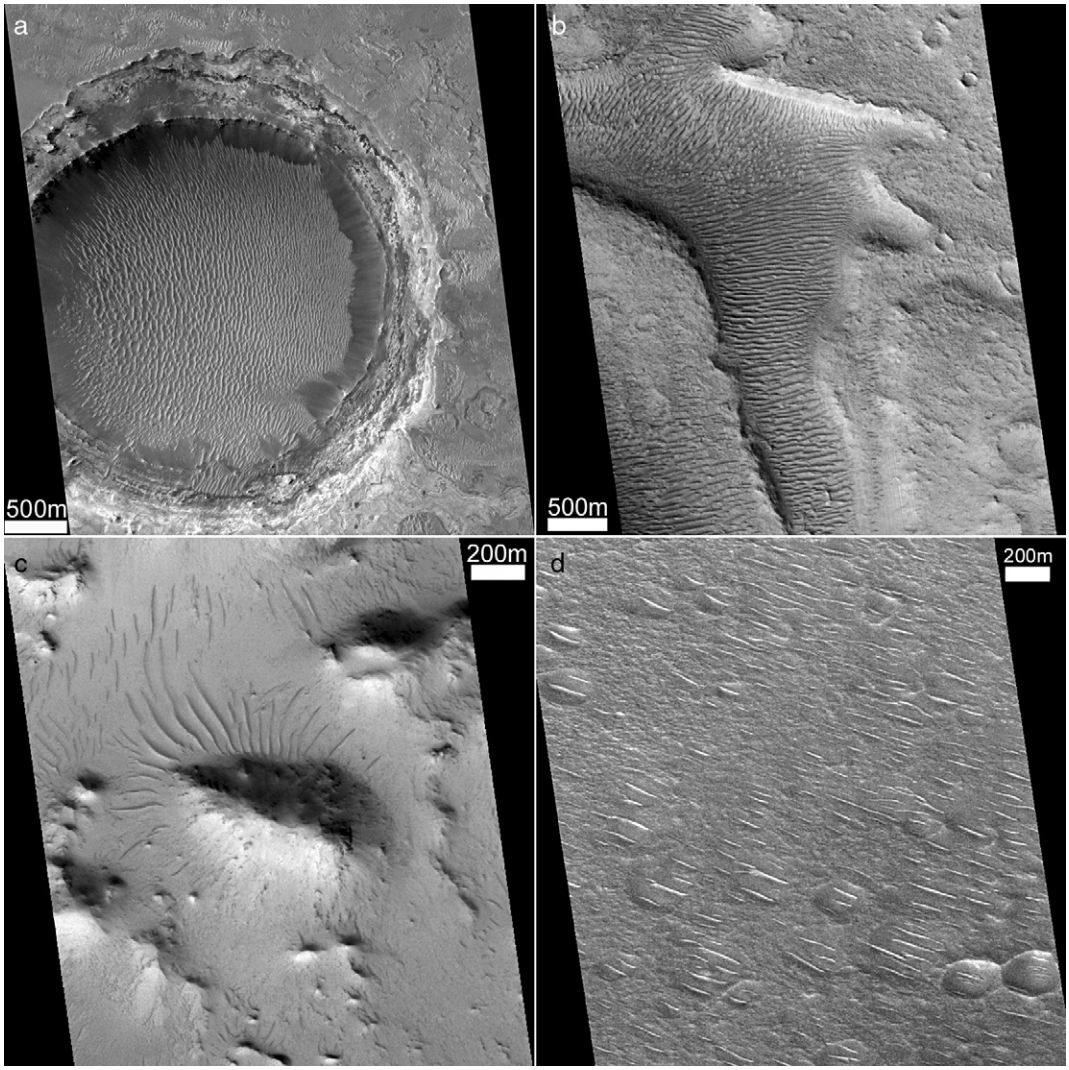

Fig. 8. Classification of TAR deposits by topographic influence. (a) Confined, at ~0.4 N., 5.4 E. MOC NA image S0100833. (b) Controlled, at ~25.9 N., 10.4 E. MOC NA image E1601902. (c) Influenced, at ~23.2 N., 7.2 E. MOC NA image M1200437. (d) Independent, at ~42.7 N., 43.9 E. MOC NA image M1003676. Image credits NASA/JPL/MSSS.

appear to show the same range of morphologies as those in smaller sets, therefore any classification by deposit size is not linked with bedform type and must be arbitrary; (ii) individual TARs within a continuous deposit can be close together (saturated; $s \sim 1$) or can be widely spaced ($s > 5$), thus deposits with the same number of similar bedforms can cover very different areas and deposits of similar area can have large differences in volume of sediment. A scheme that classifies deposit size by area might be useful for one purpose, but a scheme that classifies by number of bedforms might be more sensible for another; and (iii) remote sensing studies of Mars dominate our knowledge of TARs, thus smaller features beyond the resolution limits of the data might be missed in classifications. In terrestrial studies, initial classifications were developed from fieldwork rather than remote sensing.

For smaller TAR accumulations we have followed the line of Wilson and Zimbelman (2004) and refer to deposits of the order of tens of TARs as "TAR patches". For larger deposits, of the order of hundreds of TARs, we use the term "TAR fields". Larger deposits with thousands or more TARs or areas $> \sim 50$ km^2 we refer to as "TAR seas".

3.3. Composition and particle size

TARs and LDDs have distinct size and morphological characteristics that suggest there is an intrinsic difference in their formation process, in the materials of which they are composed, or perhaps in their age or stage of development. A number of lines of evidence suggest that TARs are made up of different types of sediments to LDDs, but whether the difference is compositional (i.e., different minerals) or physical (e.g., agglomerates versus solid grains) is unknown. For example, TARs are typically brighter than the surrounding terrain, especially where they overlie the large dunes (Malin and Edgett, 2001); and the albedo of bright TARs has been measured as >0.21, about twice that of the dark dunes (Edgett and Christensen, 1991, 1994; Edgett, 1997; Edgett and Parker, 1998). Some TARs, however, are similar in albedo or darker than surrounding terrains. Edgett (1997) suggested that the albedo of duneforms might serve as an indicator of whether they were active: 'bright' being thought to indicate 'dust covered' and hence inactive. MOC images argue against this, as there are some clear examples of bright TARs overlying dark dunes as well as dark TARs overlying brighter bedrock (although in MOC images only relative albedo can be reliably determined). Edgett and Parker (1998), Malin et al. (1998), and Edgett and Malin (2000) suggested instead that compositional difference could explain the albedo contrasts. LDDs in most regions on Mars show a mafic composition (Edgett et al., 1992), with the exception of one large erg near the north pole that shows a strong gypsum component (Langevin et al., 2005). The composition of TARs has been more difficult to measure both because spectrometry instruments have not had sufficient spatial resolution to image individual TARs and because TAR deposits are generally smaller than

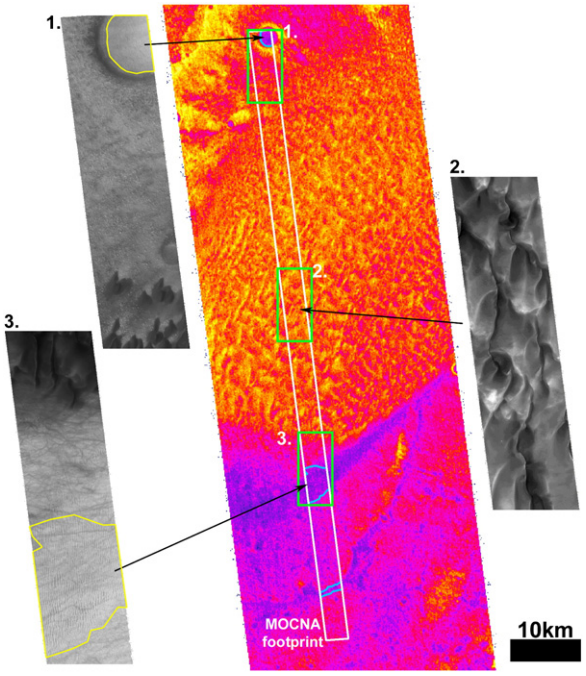

Fig. 9. Example of thermophysical properties of TARs. The main image, THEMIS night-time thermal infrared image I00967002, shows part of the Proctor Crater dunefield (approximately centered at 47.7 S 30.5 E). Red and yellow colors represent warm surface temperatures; pink and blue colors represent cooler surface temperatures. The white box shows the footprint of MOC NA image M1001334. In the MOC image, continuous TAR deposits were mapped and are shown by the yellow outlines in the MOC close-ups. When these mapped regions are matched to the THEMIS infrared image (pale blue outlines) they correspond to the coolest regions whereas the LDDs correspond to the warmest regions. This indicates that the TARs cool quicker at night than the LDDs, indicating finer particles or lack of induration. Image credits NASA/JPL/ASU/MSSS.

LDD fields and ergs. Nevertheless, Fenton et al. (2003) used Thermal Emission Spectrometer (TES) data to obtain approximate mineral compositions for LDDs and TARs, and they found approximately basaltic signatures for both and little evidence to suggest that the two types of bedforms have radically different compositions.

Although available data suggest LDDs and TARs are compositionally similar, their albedo and morphological differences might instead reflect differences in particle size or type (agglomerates versus solid grains). Remote sensing 'thermal inertia' data provide an alternative means to *in situ* sampling for probing the physical properties of TARs. The general principal of thermophysical sampling is that terrains that stay warmer at night are composed of larger particles, or have a larger fraction of bedrock, than materials that cool down quickly that are composed of fine sand or dust (Presley and Christensen, 1997a,b). Thus, thermal inertia can tell us about the size of particles in aeolian deposits. Several caveats are associated with using such data though: first, measurements integrate over a thermal skin depth that can be of the order of several centimeters deep, thus thin layers of sediments can be 'invisible' as the signal represents dominant material beneath. Also, poorly sorted or bimodal sediments can 'mix' the signal to give an average thermal inertia and hence a misleading particle size. Second, pixel sizes of thermal inertia measurements are generally larger than individual TAR bedforms and can include other surface features such as boulders, inter-bedform bedrock, or sand or dust drift deposits. Again, the result is an average thermal inertia rather than a true measurement. Finally, indurated material of fine particle sizes can have high thermal inertia, thus interpretation of thermal inertia must consider induration as well as particle size. Fenton et al. (2003) found that medium to coarse basaltic sand was the best candidate for TAR-forming materials in Proctor Crater from THEMIS thermal inertia measurements, but also found that LDDs in a similar region were likely composed of even coarser sand particles. Balme and Bourke (2005) demonstrated that TARs have lower relative thermal inertias than LDDs using THEMIS night-time images in which both TARs and LDDs were present. Zimbelman (2003) and Fenton and Mellon (2006) also found that TARs have relatively low thermal inertias compared to LDDs. In fact, TARs appear darker than LDDs in most night-time thermal images where they occur together, indicating that they have a lower thermal inertia (Fig. 9). Assuming that the mineralogy of the sediments are the same, these observations suggests three possibilities: (i) TARs are composed of smaller particles than LDDs, (ii) LDDs and TARs have similar particle sizes but in general LDDs are lithified, or (iii) TARs and LDDs have similar particle sizes but that the particles that form TARs are agglomerates, porous, or otherwise of low thermal inertia in and of themselves.

3.4. Global or latitude distribution of TARs

TARs are common on Mars and have even been found high on the Tharsis volcanoes, an elevation associated with extremely low atmospheric pressure (Malin and Edgett, 2001). No global survey of TARs has been performed to date, primarily because of the small size of

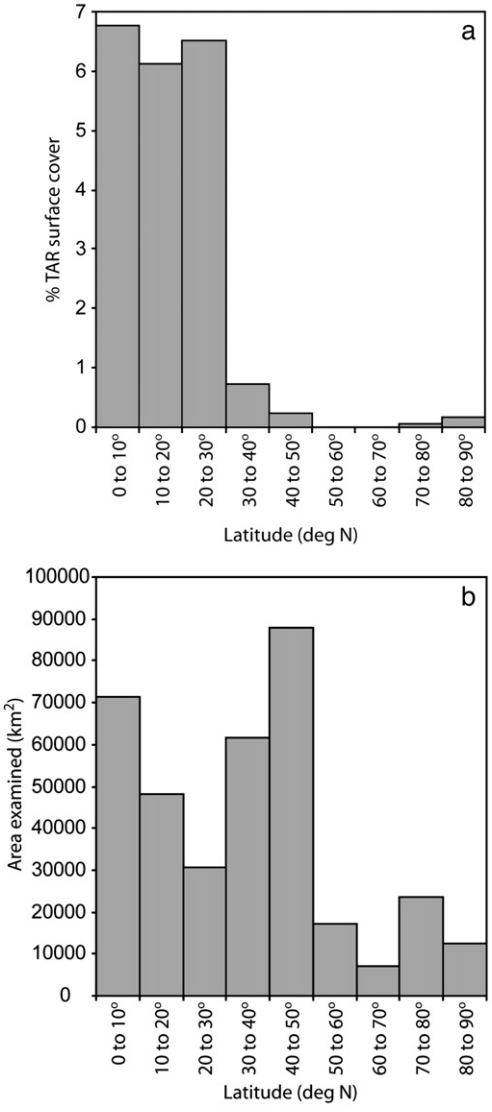

Fig. 10. Latitude dependence of TAR distributions. (a) Mean percentage TAR cover in all images studied as a function of latitude. (b) Total area studied as a function of latitude.

TARs and the limited areal coverage of high-resolution MOC NA images. In a preliminary pole-to-pole survey that examined ~5000 MOC NA images in a longitude band 180 to 240° E, Wilson and Zimbelman (2004) found that the distribution of TARs is not ubiquitous and that the percentage of MOC images containing TARs is extremely low in the northern and southern mid to high latitudes. We have performed a similar, but larger, survey that examines ~10,000 images in a pole-to-pole swath on the opposite side of the planet. Our survey also differs in that we noted the approximate areal coverage of TARs in each image, rather than simply whether an image contained TARs or not, and classified TAR deposits using the criteria discussed above.

Although only the northern hemisphere has been examined at this point, our results (Fig. 10) agree well with those of Wilson and Zimbelman (2004), showing that TARs are rare at latitudes higher than ~30° N. The low-latitude part of the northern hemisphere study region (Fig. 11) contains many images with high TAR coverage. In particular, the southwest corner has many images with almost 100% TAR coverage as well as many images with almost no TARs. This region corresponds to the eastern Terra Meridiani: a region of moderately low-lying, heavily cratered terrain that is covered by extensive, approximately horizontally-bedded deposits that have been heavily dissected and etched by wind erosion (Edgett and Parker, 1997). This region also contains the hematite-rich terrain (Christensen et al., 2000) where the Mars Exploration Rover Opportunity is currently active (Squyres et al., 2004). Because this corner of the study area has large TAR seas and is such a geologically unique environment, prior to extending the survey to the southern hemisphere, we included a new study area to the west and southwest to cover more of the Meridiani region. Fig. 11 also shows the results of this extended survey and confirms that the Meridiani region has abundant TARs. Indeed, the average TAR cover per image in the southeastern part of this extended study is nearly 50%, suggesting that the Meridiani area is a source region for TAR-forming materials.

Outside of the first-order observations of many TARs in Meridiani and the marked absence at around 30° N., are other distinct features in

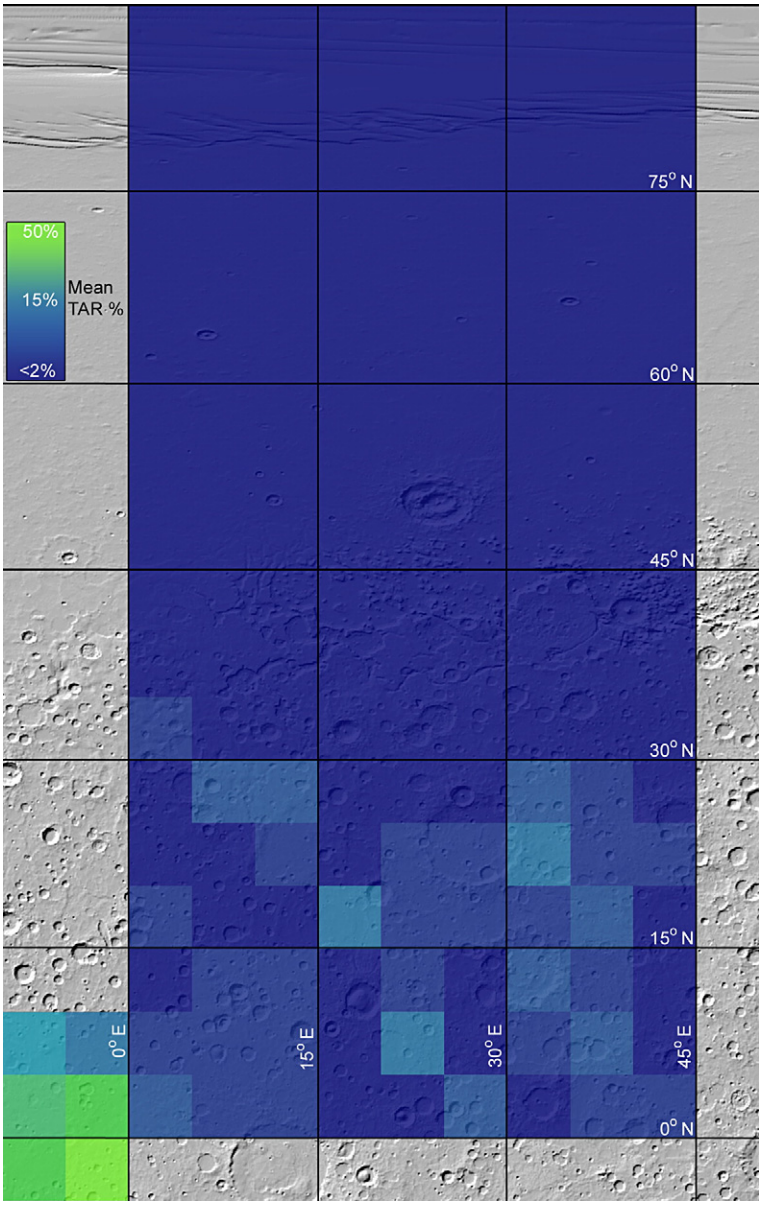

Fig. 11. Spatial distribution of TAR areal coverage. Percentile TAR coverage per image was averaged for all images over 5° by 5° bins (based upon the image centre point). The main part of the image shows the results of the northern half of the pole-to-pole survey, the small "outlier" bottom left shows the results from the Meridiani Planum region survey. The background image is a shaded relief map generated by the USGS from MOLA laser altimeter data. These data are in a simple cylindrical projection.

the TAR distribution. First, the distribution is non-random — obvious spatial clusters of images that contain TARs are present, as well as large regions in which all of the images contain no or very few TARs. Many of the images with TARs are found in impact craters, and almost all show layered terrains within a few km of the TAR deposits. In many cases, these terrains show signs of mass wasting or wind erosion, implying a local source for TAR-forming materials from eroding layers. Second, the geographical distribution of various classifications of TARs is non-random. A much higher proportion of barchan-like TARs occurs in Meridiani than elsewhere in the study area, and many of these have even lower plan view aspect ratios than other 'barchan-like' TARs outside this region. In addition, the TAR deposits in Meridiani are generally larger, more continuous, and of lower albedo than TARs outside this region. TARs in Meridiani seem, therefore, to be morphologically distinct from TARs in other regions.

3.5. Age relationships and associations with Large Dark Dunes and other features

Like all aeolian deposits on Mars, TARs are generally thought to be geologically recent, as evidenced by their often pristine morphologies and superposition relationships. Reiss et al. (2004) performed crater counts on TARs in Nirgal Vallis and found that, with a factor of two errors, they ceased to be active in that region 1.4 to 0.3 Myr before present. Zimbelman (2003) also notes cratering on TARs in this region. However, in general we have found few craters on TARs in the survey, although it must be noted that at MOC NA resolution only craters larger than 10–20 m diameter could be reliably identified. Thus while some TAR deposits are old enough to develop a population of impact craters, they are still young in the sense that they formed in the last few fractions of a percent of Mars' recorded geological history.

LDDs are also geologically recent surficial deposits, but given their larger size and greater sediment volume it would seem intuitive that the LDDs would be older. However, Malin and Edgett (2001) observed that where dark dunes and bright TARs occur together, the dunes postdate the TARs. In our study, we identified several hundred images that contained both TARs and LDDs. Of those, 67 had >5% TAR coverage and were then re-examined to determine whether TARs or LDDs were the younger bedform. LDDs clearly superposed TARs in ~66% of the images, superposition relationships were inconclusive in ~31% of the images, and in one image (~1.5%) both TARs and LDDs were the superposing bedform type in different areas of the image. TARs consistently superposed LDDs in only 1 image or 1.5% of the sample. Wilson and Zimbelman (2004) noted that in many cases TARs appear unaltered by the dark dunes that have apparently migrated across them, suggesting that the TARs are indurated or lithified. Fenton et al. (2003) also found evidence of this behavior, but suggested that in some cases the TAR bedforms are wiped out by the dark dunes, only for new TARs to form in their wake. TARs are not always older than proximal LDDs: Wilson and Zimbelman (2004) found TARs superposing dark dunes, and Fenton et al. (2003) described TAR orientations within large dune fields that have clearly been influenced by the presence of the dark dunes.

The wind conditions under which LDDs and TARs formed can be examined by comparing the orientations of their crest ridges or slip faces. Of the 67 images described above, we found that LDD and TAR crests had similar azimuths in ~57% of the images, azimuths differing by about 45° in ~15% of the images and a difference of about 90° in 13% of the images. In ~30% of the images the interpretation was inconclusive because LDDs had multiple slip faces, no slip faces, or because the TARs were networked. We found one example where the orientations of the TARs were clearly controlled by the LDDs and 1 example where the dominant crest-ridge orientations of the TARs were at 90° to the local LDD orientation but where secondary crest-ridge orientations of the TARs exactly matched the LDD orientations. There were several cases of different orientation associations in the same image, hence these numbers do not add to 100%. The results broadly follow those of other workers: Fenton et al. (2003), for example, measured orientations of TARs in Proctor crater and found that the inferred wind directions are consistent with orientations of dust devil tracks and dark dune slip faces. Thomas et al. (1999) noted that in seven out of ten unambiguous instances, the inferred wind direction from TARs matched local wind streak orientations, suggesting that TAR orientations are consistent with geologically recent winds. We have found no clear correlation with dust devil track directions; some TAR deposits are oriented perpendicular to dust devil tracks indicating a consistent wind regime while others are not.

Dust devils tracks are forming today on Mars in great numbers (e.g., Balme et al., 2003), and so observations of TARs superposing such tracks would provide strong evidence for ongoing TAR activity. However, dust devil tracks only survive on the surface for a few months (Balme et al., 2003) so it is unlikely that TARs would ever be observed to cover them, even if TARs could move very quickly when active. Slope streaks, however, are mass wasting landforms that are also actively forming on Mars today (Sullivan et al., 2001) and persist for up to tens of years (Aharonson et al., 2003). Edgett and Malin (2000) highlighted an isolated example of slope streaks superposing TARs and inferred that these TARs were inactive. To test if this observation was generally applicable, we noted those images in our survey with both TARs and slope streaks and analyzed the superposition relations. In most cases, these relationships were inconclusive (most commonly because the landforms did not overlap one another), but where a relationship could be established, slope streaks were seen to superpose TARs in all cases (Fig. 12 for example). TARs are also occasionally superposed by gully debris aprons (Malin and Edgett, 2000), some of which are also thought to be currently active (Malin et al., 2006). We have also observed several examples of TAR deposits that show orientations consistent with the dominant wind directions inferred from local yardang formations that presumably represent wind regimes that are consistent (although not necessarily active) over long periods of time. Greeley et al. (1993) found that yardang orientations in general do not correspond to present-day wind patterns. Thus if TAR orientations consistently match those of yardangs, this might be an indication that TARs did not form under the present-day wind regime. However, as Greeley et al. (1993) point out, yardang orientation can be strongly controlled by structures in the rock units, rather than dominant wind direction. Finally, some TARs are lineated, ridged, or otherwise appear eroded, indicating that

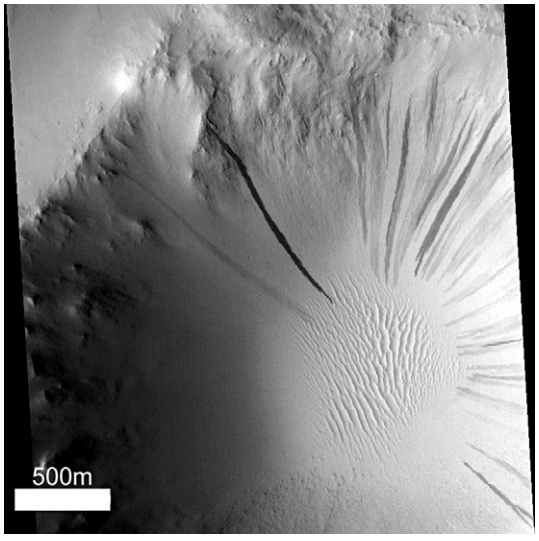

Fig. 12. Slope streaks superposing a topographically controlled patch of simple/forked TARs, at ~24.2 N., 16.7 E. MOC NA image M0203904. Image credit NASA/JPL/MSSS.

they are lithified and immobile. Such examples are rare though; most TARs have a more pristine morphology.

In short, strong evidence exists to show that TARs have a range of ages, although all are classed as 'geologically recent', but that generally they are older than LDDs, also thought to be 'recent'. Nevertheless, TARs, LDDs, and dust devil tracks often show similar inferred formation wind directions indicating either that many TARs formed under present-day wind conditions or that wind conditions have been stable in these regions for millions of years. Finally, while some TARs are clearly younger than some LDDs, the overall relation of TARs to slope streaks suggests either that they are not active today, or that they are active on a much longer timescale than slope streaks (i.e., hundreds to thousands of years rather than tens of years).

3.6. Evolution of TAR morphologies

In the Meridiani area in particular, spatial transitions downwind from merging barchan-like TARs into sinuous TARs and then into simple TARs (Fig. 13a and b) are commonly observed. Spatial transitions from saturated, sinuous, forked, and simple TARs into networked TARs (e.g., Fig. 13c) can also be seen in some regions and are particularly associated with sediment trapped in topographic lows. This response is similar to the evolution and merging of barchan dunes into barchanoid ridges on Earth (Lancaster, 1995). Close examination reveals that many of the larger simple or sinuous TARs in the Meridiani region formed from very small barchan-like TARs that have coalesced, their ridge-crest merging to form sinuous or simple bedforms. Fig. 13b shows very large TARs (the largest TARs are spaced about 80 m apart and have crest-ridge lengths of up to 400–500 m) that appear to have coalesced from smaller, saturated barchan-like TARs (the smallest are <10 m in crest-ridge length and ~10 m in wavelength).

Also visible in Fig. 13b and c are secondary ridge crests forming approximately perpendicular to the largest TAR crest ridges. Bourke et al. (2003) classified these features as an independent crest-ridge morphology they described as "feathered". The secondary crest ridges most often form perpendicular to the main crest ridges but oblique examples are not uncommon. These 'feathered' TARs are somewhat similar to networked TARs, but we suggest that networked TARs represent primary bedforms that form together in complex or multi-directional wind regimes, whereas feathered or secondary crest ridges are compound forms that develop after the primary set has become large enough to channel wind flow or where wind directions have systematically changed. Larger, primary TARs probably respond more slowly to wind changes (or might become inactive or lithified) than smaller TARs, allowing the secondary crest to form over and around them.

4. *In situ* observations of TARs

In situ observations of martian landforms are few as they require suitably instrumented landing craft such as the Viking and Mars Pathfinder landers and the Sojourner and twin Mars Exploration Rovers (MERs). Additionally, mission planners have tried to avoid close contact between a rover and meter-scale or larger aeolian deposits as such 'sand-traps' could easily snare the rover, bringing a multi-million dollar mission to a premature end. The notable exception to this rule is the MER Opportunity rover that, over the last three years, has traversed over 10 km of plains covered by meter-scale aeolian bedforms (Figs. 14a and 15) after having landed in a small impact crater (Fig. 14b) on the Meridiani plains of Mars in 2004 (Squyres et al., 2004). To reinforce the dangers of aeolian deposits to rovers, Opportunity was trapped in one of these bedforms for several weeks when its wheels became buried too deeply in the sand (Fig. 15). Opportunities' twin rover, Spirit, has also made observations of aeolian bedforms but, in general, these have been of smaller, more isolated examples than at the Opportunity site.

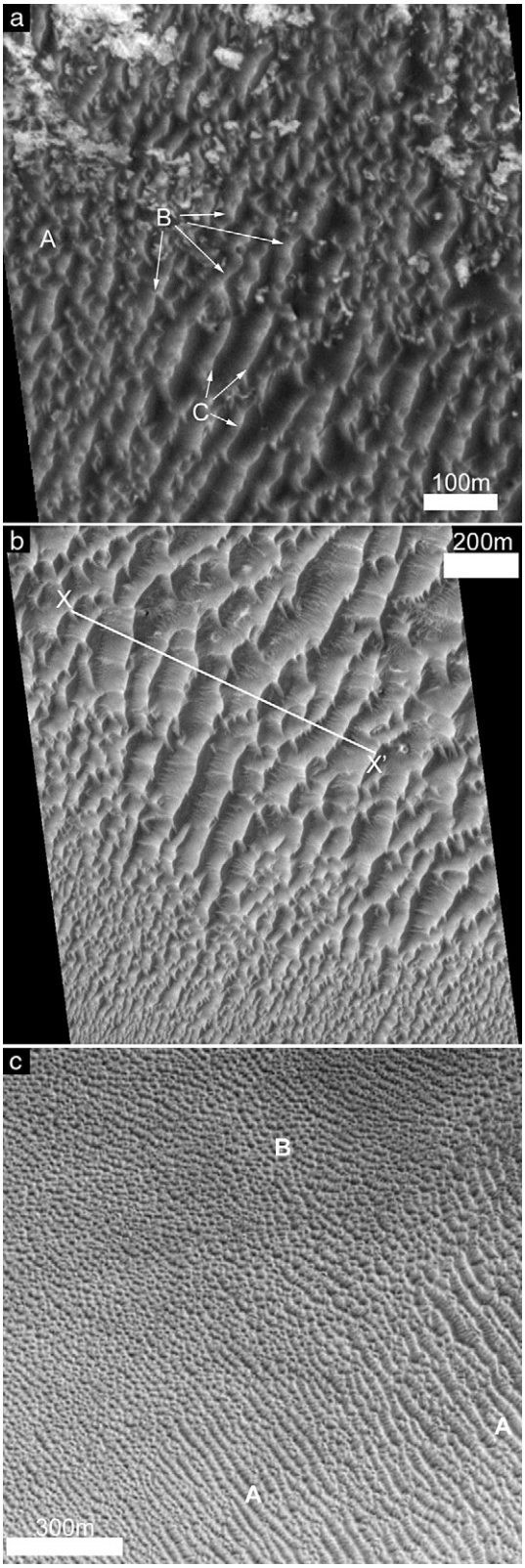

Fig. 13. (a) Example of barchan-like TARs in the Meridiani region (A) merging into sinuous (B) and simple (C) TARs. MOC NA image M1201981. (b) Very small TARs alongside very large TARs in the Meridiani region. The large TARs appear to have formed from coalescing smaller TARs and have λ~80 m. Also visible are "feathered" or secondary ridge crests. MOC NA image S0100625 (c) Simple TARs (λ~20 m) with secondary crest ridges (A) transitioning to networked TARs (B) that still show a slight trend in orientation. MOC NA image R0902119 at ~47.45 S., 36.7 E,. Image credit NASA/JPL/MSSSS.

The ripple-like bedforms that temporarily trapped Opportunity are part of a huge aeolian deposit that extends tens of kilometers across the Meridiani plains. Many of these bedforms are too small to be resolved in MOC NA images, but can be seen in HiRISE images (Fig. 14). Fig. 14 shows a continuum of size and morphology from the small ripple-like forms crossed by Opportunity to bedforms equivalent to TARs observed in MOC images. Additionally, other TAR-like deposits occur within large craters in this area (Fig. 14c and d). The bedforms on the plains are more akin to terrestrial granule ripples than dunes (e.g., Sullivan et al., 2004) because of their absence of slipfaces, low slope angles, and particle size distribution. In particular, wheel trenches reveal that the crests of these ripples are dominated by a monolayer of 1–2 mm fragments of spheroidal concretions (Sullivan et al., 2005) thought to be mainly composed of hematite (Squyres et al., 2004), but

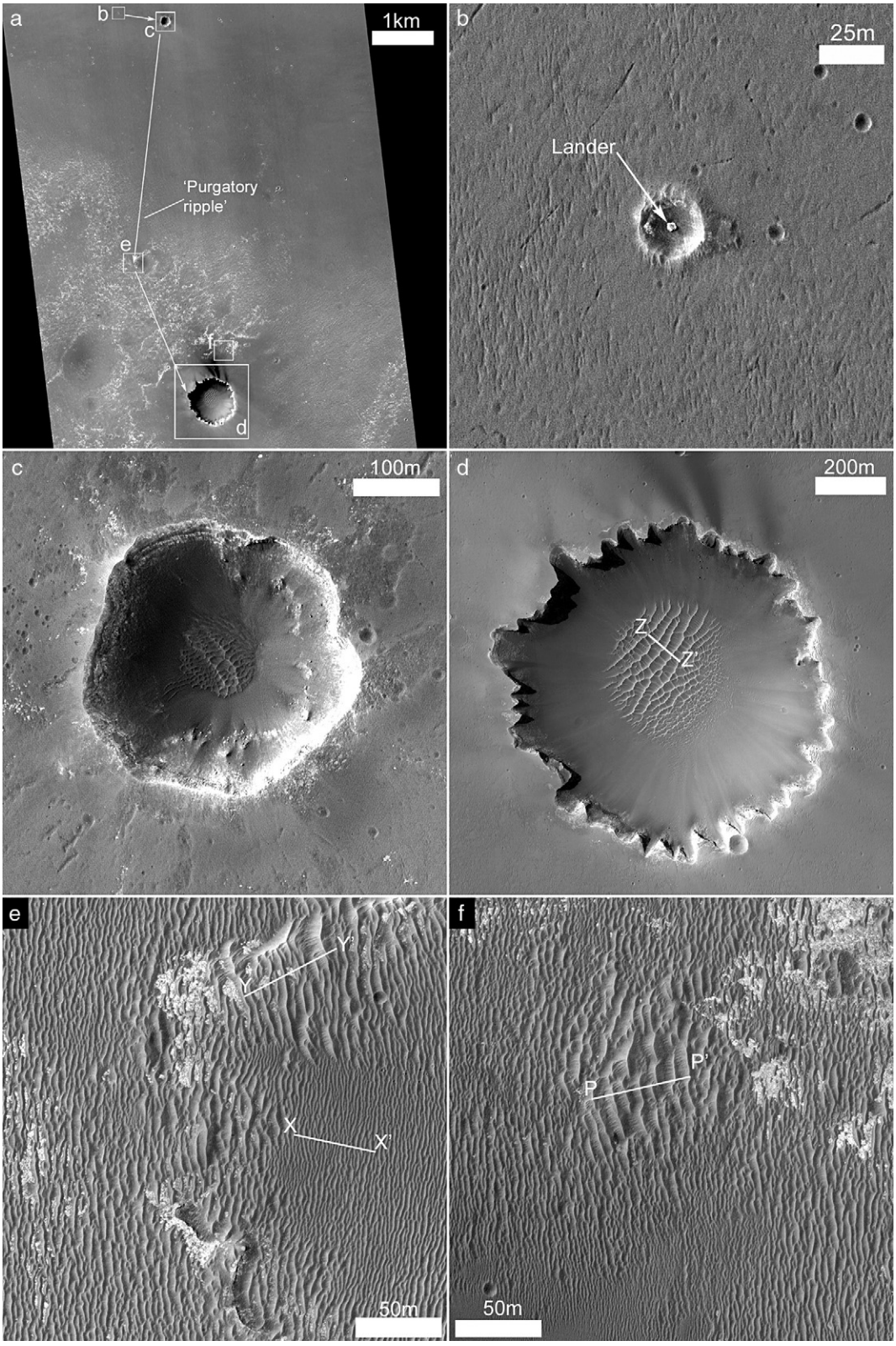

Fig. 15. Looking back at "Purgatory ripple". MER Opportunity NavCam image taken on sol (martian day) 466 of the mission. The rover was stuck in this ripple for several weeks. The ripple wavelength here is ~2.5 m; the ripples are ~30 cm high. NASA Planetary Photojournal image PIA07999. Image credit NASA/JPL.

the interior of the ripples, and the regolith in general, is composed of a poorly sorted mix of ~100 μm sand particles, dust particles and a few larger clasts (Sullivan et al., 2007). Some cohesion exists in the soil, based on observations of trench walls. Inter-ripple areas are dominated by 50–125 μm grains of basaltic sand and additional concretion fragments and intact concretions several millimeters in diameter (Sullivan et al., 2005). As the rover continued south, the bedforms became larger (as shown in Fig. 14e and f), and the observed fragments of concretions armoring the ripples became smaller (Sullivan et al., 2007). In addition to these large ripples, Sullivan et al. (2005) noted another population of smaller (~10 cm wavelength) ripples that formed almost entirely within basaltic sands trapped in local topographic hollows such as craters, pits, and troughs. These small ripples have orientations perpendicular to the current wind direction, inferred from observations of transient wind streaks from Eagle crater. The orientations of the larger ripples differ from this by between 10 and 40°, interpreted by Sullivan et al. (2005) to indicate a shift in wind regime and evidence of the larger bedforms being relatively inactive. Jerolmack et al. (2006) estimated wind strengths required to create dust streaks and activate the ripples in this region. They found that surface friction wind speeds (u^*) of ~3.5 m s^{-1} (equivalent to ~70 m s^{-1} winds at 1 m height) are required to activate the granule ripples, about twice the wind speed required to create the transient wind streak. From this they suggest that the ripples might have been active in the last decade. In contrast, using analog field studies of the rate of granule ripple movement at Great Sand Dunes National Park and Preserve, USA, Zimbelman et al. (2007) suggested that the MER ripples are ancient and have not been recently active. Similarly, Sullivan et al. (2007) showed that ejecta blocks emplaced onto the ripples have eroded to conform to the ripple surface, indicating that this erosion occurs more quickly than the ripples can actually move. These observations strongly suggest that the granule ripples are only rarely active.

The two largest craters visited by Opportunity — Endurance and Victoria — contain aeolian bedforms similar in planform morphology to TARs (Figs. 14c and d, 16 and 17). Both sets of TARs in these craters show crest-ridge morphologies transitional between simple and networked and have clear secondary crest ridges. Sullivan et al. (2007) noted that the ripples in the southern part of the Opportunity traverse also showed evidence of secondary crest ridges, although at a smaller scale. Squyres et al. (2006) interpret the Endurance Crater bedforms to be a combination of small star-dunes and large ripples (Figs. 14c and 16).

5. Discussion

5.1. Terrestrial analogs to TARs: dunes or granule ripples?

Broadly speaking, terrestrial transverse dunes and granule ripples are distinguished from one another by their scale, and by morphological and textural differences. For example, although terrestrial granule ripples with wavelengths of up to ~20 m (Bagnold, 1941) or even ~30 m (Malin, 1986) have been observed, they generally have shorter wavelengths of several meters (e.g., Wilson, 1972; Fryberger et al., 1992; Zimbelman and Williams, 2007). Transverse dunes, however, can have wavelengths of tens to thousands of meters (e.g., Lancaster, 1995; pp 54–59). In terms of morphology, dunes individually alter the local airflow, leading to flow separation zones, angle of repose slip faces and slip face avalanching. They also commonly have smaller aeolian bedforms (such as smaller dunes, granule ripples or aerodynamic ripples) superposed upon them. In contrast, granule ripples are generally not large enough to affect the local winds, have below angle of repose slipfaces, and rarely show smaller, aerodynamic ripples superposed upon them. Granule ripples are also distinguished by their texture (e.g. Wilson, 1972), having concentrations of large sand or granules at the surface (and especially at their crests), and fine grained or poorly sorted material within. This contrasts with dunes, which are well-sorted to very well-sorted in coastal environments and moderately sorted to well-sorted in inland environments (Ahlbrandt, 1979).

Although TARs seem too large to be granule ripples, given that terrestrial examples with wavelengths greater than a few meters are rare, calculations by White (1979) suggested that the kinetic energy of sand grains in saltation on Mars can be an order of magnitude greater than saltating particles on Earth. Thus, saltating grain impacts will create higher energy reptating particle populations. Given that Mars' gravity is about a third that of the Earth's, these particles will therefore have longer mean reptation lengths. Additionally, grain impacts will cause more severe creep if the impacted particles are too large to be moved by reptation, and larger particles will be able to be moved by creep than on Earth. Assuming that the process that governs the scaling of granule ripple wavelength is indeed reptation/creep (e.g., Anderson, 1987; Ungar and Haff, 1987; Yizhaq, 2004), the maximum

Fig. 14. HiRISE image PSP_001414_1780_RED, showing a part of the Meridiani plains where the Opportunity Rover is operating. HiRISE images can have spatial resolutions as good as 25 cm/pixel, allowing sub-meter-scale landforms to be studied. (a) The approximate path of Opportunity across the Meridiani plains from its initial landing site inside "Eagle" crater (b) to its current location on the rim of "Victoria" crater (d). (b) Eagle crater, still showing the landing craft that carried the rover to the surface. North–south orientated ripples are visible around the crater. These were observed by Opportunity to be a few tens of centimeters across, up to a few meters wide and a few centimeters in height. (c) Endurance crater containing small aeolian bedforms. The rover entered this crater and imaged this deposit from the surface (Fig. 16, below). In earlier, low resolution images, the crater appeared to contain two or three small, simple TARs. Higher resolution and surface images show a complex suite of small TARs with a barely dominant ridge-crest orientation and strong secondary ridge crests. (d) TARs within the larger Victoria crater. This deposit would be described as a topographically confined, networked TAR patch in our remote sensing classification. At the time of writing, the rover has not yet entered Victoria crater, but has imaged the sediments from the crater rim (Fig. 17). The TARs here have a spacing of ~30 m (Z–Z′), similar to networked TARs around Mars. (e) As the Rover traveled south, the ripple-like bedforms generally became larger. Here, on the rim of a subdued crater named 'Erebus' the larger bedforms (Y–Y′) have λ ~ 6 m. The smaller bedforms within the crater (X–X′) have λ ~ 2.5 m and are more typical of the northern part of Opportunity's traverse. (f) North of Victoria crater are the largest bedforms in the HiRISE image (λ ~ 10 m; P–P′). These show identical morphology to merging barchan-like TARs observed in MOC NA images in other parts of Meridiani. Image credit NASA/JPL/UofA.

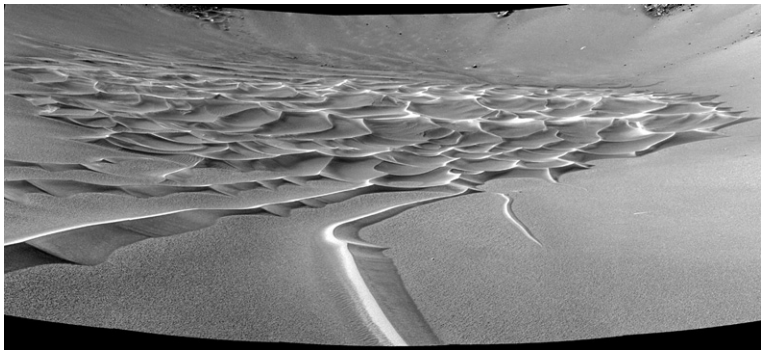

Fig. 16. Looking east toward the small TAR patch within Endurance crater. The primary ridge crests (perpendicular to viewing direction) have λ ~ 20 m. The secondary ridge crests (approximately parallel to viewing direction) have λ ~ 3–6 m. Grey scale version of a part of a false-color mosaic of MER Opportunity PanCam images taken on sol 221. Image mosaic Sol211B_P2424_L257F from http://pancam.astro.cornell.edu/pancam_instrument/. Image credit NASA/JPL/Cornell.

wavelength of granule ripples could therefore be much greater on Mars than on the Earth. This would then lead to similarities in wavelength between large ripples and small dunes. For example, Yizhaq (2005) found that a supply of particles with saltation path lengths of ~ 10 m could result in ripple wavelengths of tens of meters on Mars: a figure within the wavelength domain of small transverse dunes on Earth. Thus calculations suggest that a simple scale argument is insufficient to distinguish between a granule ripple and dune genesis for TARs.

The origin of TARs might therefore best be determined by measurements of particle size distribution or by detailed morphological studies. This process has already begun using data returned by the Opportunity rover. These images show bedforms in the Terra Meridiani region that have no obvious slip face and contain poorly sorted interior particles armored by larger granules. These observations parallel the morphology and descriptions of "the poured-in" texture found for granule ripples in Namibia by Fryberger et al. (1992). In addition, the ripples at the Opportunity site form the smallest examples of a large deposit of such bedforms, the largest having morphologies and sizes consistent with MOC NA observations of TARs. As shown in Figs. 13 and 14, continuum in form exists between the largest and smallest bedforms, thus this is strong evidence that even the largest examples are granule ripples and not dunes.

This is not to say that all TARs are granule ripples. The Meridiani TARs are morphologically different in many respects from TARs in other areas. In addition, within the Victoria and Endurance craters in Meridiani are confined, networked TAR patches that are morphologically different from TARs on the surrounding plains and appear to be more similar to TARs in other regions. Also, Sullivan et al. (2007) noted that the larger bedforms in Meridiani were armored with smaller fragments of concretions. Thus, while we suggest that many Meridiani TARs are likely to have formed as granule ripples, TARs in other regions might still have formed as small transverse dunes. Additionally, it should be noted that small transverse dunes and large granule ripples are not the only potential terrestrial analogs for TARs. "Zibars", low relief, transverse aeolian bedforms with wavelengths of tens to hundreds of meters (e.g., Lancaster, 1995; pp 78–81) that form on sand sheets and in inter-dune corridors in terrestrial sand seas, might also be good analogs for TARs. Zibars do not have slipfaces or defined crests, and have shallow slopes. However, little is known about the morphometry or even the origin of terrestrial Zibars, so any comparison with martian TARs remains speculative.

Although *in situ* textural measurements seem to be the most powerful method to discriminate between dunes and granule ripples on Mars, a lack of surface missions prevents such analyses in more than a handful of regions on Mars. Nevertheless, new HiRISE data — especially topographic profiles of TARs made from stereo or photometric methods (e.g., Zimbelman and Williams, 2007) — are becoming available, and will provide the best alternative method to compare TARs with terrestrial analogs.

5.2. Sediment source and spatial distribution

On Earth, aeolian dunes and ripples form from sand-sized, or granule-sized, sediment that has been transported, concentrated, and remobilized by the action of water, wind, or ice. The origins of dune sand are usually found in sandstone deposits or alluvial or littoral sediments, and sediment pathways can often be identified that link a dune deposit with a sediment source. In the case of inland dune fields, these are often upwind of eroding sandstones or alluvial, fluvial, glacial, or lacustrine sediments. Thus, terrestrial dunes are usually associated with specific source environments, and their distribution is controlled by prevailing wind patterns and topography. In contrast, few studies of sediment sources and transport pathways have been made for martian TARs. Thomas et al. (1999) suggested that TARs form only a few kilometers from their source material, and they identified bright outcroppings near

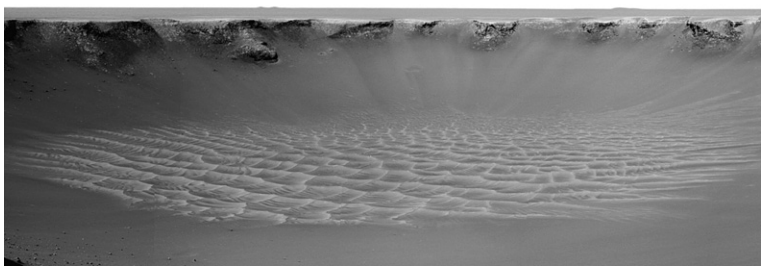

Fig. 17. Looking southeast toward the networked TAR patch within Victoria crater. The dominant NE–SW trending ridge crests are obvious, as well as approximately perpendicular secondary ridge crests. Also visible are even smaller (tertiary?) ridge crests in the inter-TAR areas that are oriented parallel to the primary ridge crests. This indicates an evolving control of local wind directions by the growing TAR deposit. Grey scale version of a part of a false-color mosaic of MER Opportunity PanCam images taken between sols 970 and 991. Image mosaic Sol991B_Cape_Verde_L257F from http://pancam.astro.cornell.edu/pancam_instrument/. Image credit NASA/JPL/Cornell.

TARs in several cases that might be the sediment source. Fenton et al. (2003) found no clear sediment pathway of high albedo material into the ~100 km diameter Proctor crater, and conclude that the high albedo TARs that form there are somehow sourced from material inside the crater. In this study, we have shown that in addition to this hypothesized control by local sediment source there is also clearly a regional and latitudinal control of TAR distribution.

To deal with regional controls first, the high concentration of TARs in the Terra Meridiani region is clearly linked to the erosion of layered sediments there (Edgett and Parker, 1997). Exposed sedimentary outcrops show a variety of morphologies consistent with erosion of friable bedrock in both orbital (Presley and Arvidson, 1988; Hynek et al., 2002) and rover images (Thomas et al., 2005). These layered terrains superpose ancient, dissected cratered highlands to the south and have been interpreted as volcaniclastic (Hynek et al., 2002), marine (Edgett and Parker, 1997), or a combination of fluvial, aeolian, lacustrine, and evaporite sediments (Arvidson et al., 2006). We suggest that weathering, wind abrasion, and mass wasting have liberated or formed sand-size particles from these lithified sediments, and that this material supplies the extensive TARs in this region. In addition, many of the MOC NA images outside this region with more than 10% TAR cover also show layered terrains, or at least significant outcrops with steep slopes that might be susceptible to mechanical weathering and mass wasting (e.g. Figs. 1d and 18). It is logical to infer that TAR-forming sediment here also form by erosion of sedimentary deposits, supporting the suggestion that local exposures of layered bedrock plays an important role in the distribution of TARs.

In terms of the latitudinal distribution of TARs, we note that our results closely match those of Wilson and Zimbelman (2004) from a study on the other side of the planet. This suggests that the latitudinal distribution may be a global pattern. Three variables might explain this distribution: (i) sediment source, (ii) sequestration of sand-size sediment, and (iii) wind regime. TARs seem to form adjacent to steep slopes and layered terrains, so the first line of enquiry is to examine topography, and how it relates to TAR distribution, especially given that Mars' terrain is divided into rugged impact-cratered highlands in the south and smoother, low-lying plains in the north. Wilson and Zimbelman (2004) suggested that kilometer-scale roughness gives the best correlation with TAR distribution, roughness serving as a proxy for abundance of steep slopes and bedrock exposures that could be sources of TAR sediments. While it is true that north of 50° latitude much of our study area is gently undulating, hummocky plains terrain with few over-steepened slopes and little evidence of erosion of layered terrains, between 30 and 50° N. the terrain is as rough on the kilometer scale as near the equator and yet we have observed few TARs. The same trend is found for the distribution of impact craters, a possible alternative source of sand-size particles (Melosh, 1989). These observations suggest that while there may be naturally fewer TARs in the higher latitude northern plains than in the southern highlands because of the paucity of steep slopes and associated mass wasting or aeolian erosion, this is not the whole story as the mid-latitudes are similar in gross geomorphology to the low-latitudes, but without TARs.

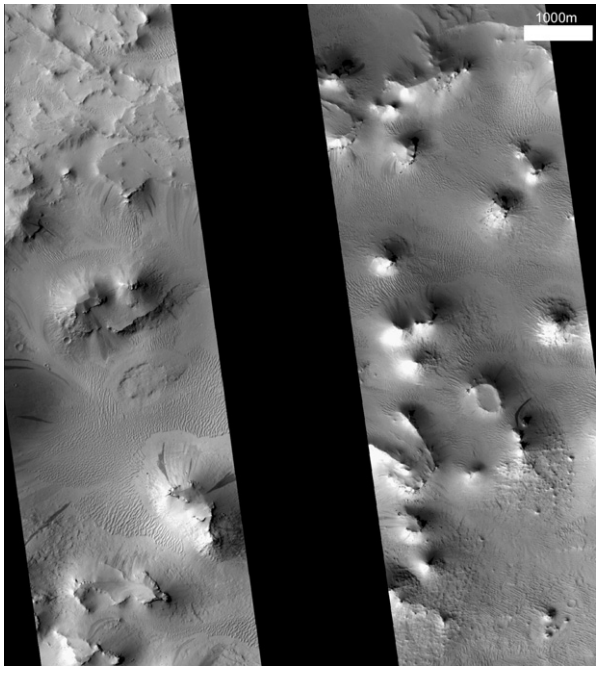

Fig. 18. Example of TAR fields associated with eroding mesa-like landforms and layered terrain at ~17.7 N, 19.3 E. Mass wasting of the layered terrain is the likely source of the sediments that form the TARs. Also visible are many slope streaks that might also be supplying TAR material. MOC NA image M001654 (left) and R0900574 (right). Image credit NASA/JPL/MSSS.

The second aspect to consider is sequestration of sand-size particles. Gamma Ray Spectrometer and Neutron Spectrometer (GRS/NS) observations of regolith at latitudes >50–60° show substantial amounts of water ice within a few tens of centimeters of the surface (Boynton et al., 2002; Feldman et al., 2004). The soils may therefore have had a degree of cohesion from ice cement holding the grains together, resulting in little mobile sediment available for transport by the wind. However, GRS/NS observations show less water content in the mid-latitudes than farther south near the equator, yet TARs are nearly as uncommon here as they are north of 50°. Another hypothesis that is also related to the near-surface of the martian regolith is that sand-grade material might be buried by centimeter — or meter-scale deposits of a dust — and ice-rich mantling material. This mantle, almost pervasive at >60° latitudes in both hemispheres but transitioning to a dissected, discontinuous mantle at 30–60° latitude (Mustard et al., 2001; Kreslavsky and Head, 2002; Head et al., 2003) is partly responsible for topographic smoothing at sub-kilometer scale at latitudes >30° in both hemispheres (Kreslavsky and Head, 2000). It is interpreted to be composed of water ice condensed from the atmosphere that includes and is overlain by fine air fall dust. The mantle is geologically very recent and is thought to be deposited and removed cyclically as a result of episodic climate change driven by orbital dynamics, in particular variations in the obliquity of Mars rotation (Laskar et al., 2004). This hypothesis is compelling in that the total latitudinal extent of the mantle is very well anti-correlated with the TAR distribution. However, the mantle is discontinuous in mid-latitudes and, unless substantial induration of sand particles somehow occurs under the mantle when it is at its fullest extent, or if the formation time of TARs is longer than the time since the mantle began to degrade, it is unclear as to why potential TAR-forming material in the mid-latitudes does not form TARs in those areas where the mantle has been removed.

The final variable is wind regime and how this might control the latitudinal variations of TARs. The observed distribution could result from a situation where mid- and high-latitude winds are too weak to move sediments and thus no bedforms are produced, or that winds are so strong that available sediment is moved rapidly away to regions where lower wind speeds allow deposition and formation of aeolian bedforms. The first scenario is not well-supported by Global Circulation Models (GCM) of Mars' atmosphere, even under different obliquity conditions (Haberle et al., 2003): the mid to high latitudes appear to be the regions with the greatest potential for sediment transport, rather than the least. The second scenario is supported somewhat by GCM models, in that at low (15°) and high (45–60°) obliquity the annual deflation potential (a model parameter linked to surface wind shear) is highest in the mid and mid-to-high latitudes (Haberle et al., 2003). However, the models suggest very low annual deflation rates at latitudes >60° for all obliquity values and thus we should expect TARs to accumulate here if sediments were indeed preferentially transported away from the mid-latitudes. This is not the case.

We suggest that the low-latitude TAR distribution is linked closely to sources of sediment (eroding layered terrain), but further investigation is required to determine the controls on the latitudinal distribution presented here. A combination of sediment availability and wind regime seems to be the most likely control on the present-day distribution of TARs.

5.3. Age and bedform mobility

Observations of impact-cratered TARs (Reiss et al., 2004) and lack of supporting superposition relations suggest that most TARs are not active today, and in general, they do not appear to be the most recent of aeolian bedforms found on Mars. However, they have a complex relationship with LDDs: in some regions overlying or being influenced by LDDs, but in most cases being superposed by LDDs. These relationships indicate that the TAR-forming materials are generally less mobile than LDD materials. This is a slightly counter-intuitive conclusion for two reasons: (i) LDDs are orders of magnitude larger than TARs, and terrestrial experience suggests that larger bedforms migrate more slowly than smaller ones (Bagnold, 1941; Gay, 1962); and (ii) the thermophysical properties of TARs suggest that, given that they are of similar composition to LDDs, they are composed of finer particles, again suggesting that they, not LDDs, should be the more mobile bedform.

The Mars Exploration Rover Opportunity found that the regolith in the Meridiani region was a poorly sorted mix of fine basaltic sand and hematite granule-sized concretion fragments (Sullivan et al., 2005), and the Spirit rover also observed granule-coated ripples where the granules were comprised of rounded rock fragments (Greeley et al., 2004, 2006). Where the regolith was worked into ripples, a monolayer of fragments was often seen on the ripple crests, with basaltic sands on the flanks, and whole concretions or other clasts mixed with basaltic sands in the inter-ripple zones. Thus, measurements of temperature made with instruments that have relatively coarse resolution, such as TES or THEMIS, would average over many ripples and inter-ripple areas and would also be sensitive to the 'average' thermal inertia of the upper thermal skin depth layer (up to a few centimeters), rather than the topmost monolayer. Thus, the remotely sensed particle size may not represent the armoring monolayer of granules that stabilize the ripples in place. We therefore suggest that many TARs are armored by granule-sized fragments and this is why they are relatively immobile compared to LDDs, inferred to be composed of better-sorted coarse sand.

Almost the only environment where TARs are reliably observed to form contemporaneously with, or after, LDDs is within LDD fields. If TARs are armored with granules, their mobility within LDD fields might be a result of funneling of winds to produce shear stresses large enough to mobilize granule-sized particles within the dune fields, or it might instead be a product of an increased supply of coarse, saltating sand that can mobilize the TAR granules by reptation or creep. This interpretation is supported by thermal infrared observations of TARs within the Proctor Crater LDD field (Fenton and Mellon, 2006) that showed that TARs here have a higher thermal inertia (more similar to that of the LDDs) than TARs outside the LDDs. This suggests either that the TARs are kept free of dust (that might usually lower their thermal inertia) by saltating sand, or that LDD sand accumulates on or within the TARs and artificially raises the thermal inertia.

Zimbelman et al. (2007) have observed similar behavior on Earth during the passage of a particularly strong storm front over the Great Sand Dunes National Park and Preserve (GSDNPP) in southern Colorado. When the documented movement was compared to wind data for the event from a nearby airport, the granule movement occurred during a 23-hour period when the average wind speed for this entire period was ~9 m s^{-1}, which is ~1.8 times the wind speed needed to initiate saltation; photographs documented the volume of granules that crossed the crest of the granule ripples during this period. Values of the atmospheric density and the acceleration of gravity on Mars indicate that the sand flux (which represents the driving force for granule movement through impact creep) on Mars should be ~3.8% of the sand flux on Earth, all other factors remaining constant. Under these conditions, the GSDNPP granule movement rate can be used to estimate that a 25 cm high granule ripple on Mars (comparable to those observed in images from MER Opportunity; Sullivan et al., 2005) would require ~175 Earth-hours (7.3 Earth-days) to move only 1 cm if the wind blew continuously during that time at an average of ~1.8 times the saltation threshold (Zimbelman et al., in review). Higher wind speeds would decrease the time required, but it is unreasonable to expect winds above threshold to blow continuously for hours, let alone days, on Mars. The conclusion is that thousands of years of more typical wind conditions would be required for martian granule ripples to move a measurable amount (e.g., one-half of the ripple wavelength) under current atmospheric conditions.

5.4. Utility of the classification scheme

In terms of facilitating the survey and simplifying tasks, such as plotting azimuthal orientations of topographically independent TAR deposits, the new classification scheme has been very successful. We have been able to filter the extensive dataset by these classification criteria to study different aspects of TARs; for example, the higher abundance of barchan-like TARs in the Meridiani region than elsewhere, which perhaps indicates a different formation mechanism, sediment type or supply, or degree of evolution of the deposits. Also, identifying varying degrees of topographic control has been important for understanding whether a region with TARs is dominated by transport or capture of TAR-forming materials. We will also use these data when comparing orientation of TARs with climate models in future studies.

Although we have not yet fully explored correlations between various morphologies and morphometry or geographic locations, the combination of crest-ridge morphology classification and morphometric data has already been useful. For example, widely spaced, barchan-like TARs appear to be at one end of a sediment supply/wind regime spectrum; and closely-spaced, networked TARs at the other. However, we do not yet know how forked, sinuous, and simple TARs are related to one another; nor what the role is of inter-bedform spacing as a control on morphology. Further study of the correlation of spacing, plan view aspect ratio, and crest-ridge classification are required and might find more utility in rejecting the current division of simple, forked, and sinuous TARs in place of a morphometric criterion. In summary, the classification scheme is very useful both for describing TAR deposits in a consistent manner and also for facilitating more in-depth research topics.

6. Conclusions

(i) TARs are abundant but not ubiquitous. They preferentially form proximal to friable, layered terrains such as those found in Meridiani. Additionally, TAR distribution in the northern hemisphere shows a strong latitudinal dependence; very few TARs are found north of ~30° N. in the study region. No clear correlation exists between this distribution and Mars' gross morphology, but the best explanation seems to be a combination of (1) a lack of sediment supply in the northern lowlands because of a lack of steep slopes and outcrops of layered, sedimentary terrain; (2) a sequestration of TAR-forming materials by a periodically emplaced ice-rich mantle; and (3) possible wind regime effects driven by obliquity changes in the geologically recent past.

(ii) Remote sensing measurements of the thermophysical properties of TARs consistently suggest that TAR materials have smaller particle sizes than LDDs, yet observations show that in

most cases TARs are less mobile than LDDs. The particle size observations likely reflect both vertical and horizontal averaging of the thermal properties as the perceived particle size is not representative of Mars Exploration Rover Opportunity observations that TARs have a strongly bimodal particle size. Thus, TARs likely consist of a core of fine material armored by a monolayer of granule-sized particles that hinders TAR movement under the current wind regime in settings other than within LDD fields, where the saltation flux of finer sands is high enough to move the granules (and hence the TARs) by reptation/creep.

(iii) That TARs are essentially inactive is confirmed by superposition relations with slope streaks and LDDs and by observations of superposed impact craters.

(iv) Observations in the Terra Meridiani region by the Opportunity rover suggest that small aeolian bedforms here are ripples and not small dunes. These small bedforms trend into larger features that have similar morphologies when observed in new HiRISE images and are essentially identical to TARs observed in MOC NA images in this area. This suggests that TARs, in the Meridiani area at least, are ripples and not dunes.

(v) We have devised a new classification scheme for TARs based upon (1) crest-ridge morphology, (2) influence of topography on the TAR deposit, and (3) the size of the TAR deposit. The scheme has proved useful for both descriptive purposes and for facilitating science studies of TARs.

7. Future work

This work is ongoing and we are continuing the study to extend the TAR survey to the southern hemisphere. This will complete the survey and demonstrate whether the anti-correlation of TAR distribution with the icy mantling terrain (which exists in the south as well as the north) is valid. In addition, we have begun to map azimuthal orientations of TAR seas that are independent of topography to compare TAR azimuths with GCM wind direction data for both the current climate and conditions of higher and lower obliquity. For one or two regions (likely the Terra Meridiani and one other), we will compare TAR distribution and orientations with local wind regimes, generated using very high-resolution mesoscale climate models.

An unforeseen aspect of this work that we plan to pursue in the future is the morphological differences between TARs in Meridiani and those in other areas. We will examine TARs in Meridiani and elsewhere and make a statistical sampling of wavelength, crest-ridge length, and TAR width. From these data we will extract inter-bedform spacing and plan view aspect ratio and investigate whether different spatial populations of TARs can be correlated with morphometric populations.

Finally, as more 25 cm/pixel HiRISE data become available, we will examine these images for detailed morphological studies of TARs and perform rudimentary age dating from impact crater statistics. In addition, HiRISE stereo images (~1–2 m resolution) or photoclinometry will allow numerous cross sections for TARs to be extracted. This will provide important data for comparison with terrestrial analog studies (e.g., Zimbelman and Williams, 2007).

Acknowledgements

This work was supported by the NASA Mars Data Analysis Program through grant number NNG05GQ74G. The authors thank Lori Fenton, John Pelletier and two anonymous referees for their constructive reviews of this paper.

References

Aharonson, O., Schorghofer, N., Gerstell, M., 2003. Slope streak formation and dust deposition rates on Mars. J. Geophys. Res. 108 (E12). doi:10.1029/2003JE002123.

Ahlbrandt, T.S., 1979. Textural parameters in aeolian deposits. In: McKee, E. (Ed.), A Study of Global Sand Seas. US Geological Survey paper, vol. 1052, pp. 21–52. Washington.

Anderson, R.S., 1987. A theoretical model for aeolian impact ripples. Sedimentology 34, 943–956.

Arvidson, R., Poulet, F., Morris, R.V., Bibring, J.-P., Bell, J.F., Squyres, S.W., Christensen, P., Bellucci, G., Gondet, B., Ehlmann, B.L., Farrand, W.H., Fergason, R.L., Golombek, M., Griffes, J.L., Grotzinger, J., Guiness, E.A., Herkenhoff, K., Johnson, J.R., Klingelhöfer, G., Langevin, Y., Ming, D., Seelos, K., Sullivan, R., Ward, J.G., Wiseman, S.M., Wolff, M.J., 2006. Nature and origin of the hematite-bearing plains of Terra Meridiani based on analyses of orbital and Mars Exploration Rover data sets. J. Geophys. Res. 111 (E12S08). doi:10.1029/2006JE002728.

Bagnold, R.A., 1941. The Physics of Windblown Sand and Desert Dunes. Methuen, London.

Balme, M.R., Bourke, M.C., 2005. Preliminary results from a new study of Transverse Aeolian Ridges (TARs) on Mars. LPSC XXXVI [CDROM], Abstract # 1892.

Balme, M.R., Whelley, P.L., Greeley, R., 2003. Mars: dust devil track survey in Argyre Planitia and Hellas Basin. J. Geophys. Res. 108. doi:10.1029/2003JE002096.

Bourke, M.C., Wilson, S.A., Zimbelman, J.R., 2003. The variability of TARs in troughs on Mars. LPSC XXXIV [CDROM], Abstract # 2090.

Bourke, M.C., Balme, M.R., Beyer, R.A., Williams, K.K., Zimbelman, J., 2006. A comparison of methods used to estimate the height of sand dunes on Mars. Geomorphology 81 (3–4), 440–452.

Boynton, W.V., Feldman, W.C., Squyres, S.W., Prettyman, T.H., Brückner, J., Evans, L.G., Reedy, R.C., Starr, R., Arnold, J.R., Drake, D.M., Englert, P.A.J., Metzger, A.E., Mitrofanov, I., Trombka, J.I., d'Uston, C., Wänke, H., Gasnault, O., Hamara, D.K., Janes, D.M., Marcialis, R.L., Maurice, S., Mikheeva, I., Taylor, G.J., Tokar, R., Shinohara, C., 2002. Distribution of hydrogen in the near surface of Mars: evidence for subsurface ice deposits. Science 297 (5578), 81–85.

Christensen, P., Bandfield, J.L., Clark, R.N., Edgett, K.S., Hamilton, V.E., Hoefen, T., Kieffer, H.H., Kuzmin, R., Land, M.D., Malin, M.C., Morris, R.V., Pearl, J.C., Pearson, R., Roush, T., Ruff, S.W., Smith, M.D., 2000. Detection of crystalline hematite mineralization on Mars by the Thermal Emission Spectrometer: evidence for near-surface water. J. Geophys. Res. 105 (E4), 9623–9642.

Cutts, J.A., Smith, R.S.U., 1973. Aeolian deposits and dunes on Mars. J. Geophys. Res. 78, 4139–4154.

Cutts, J.A., Blasius, K.R., Briggs, G.A., Carr, J.R., Greeley, R., Masursky, H., 1976. North polar regions of Mars: imaging results from Viking 2. Science 194, 1329–1337.

Edgett, K.S., 1997. Aeolian dunes as evidence for explosive volcanism in the Tharsis region of Mars. Icarus 130, 96–114.

Edgett, K.S., Christensen, P., 1991. The particle size of martian aeolian dunes. J. Geophys. Res. 96, 22,765–22,776.

Edgett, K.S., Parker, T.J., 1997. Water on early Mars: possible subaqueous sedimentary deposits covering ancient cratered terrain in western Arabia and Sinus Meridiani. Geophys. Res. Lett. 24 (22), 2897–2900.

Edgett, K.S., Parker, T.J., 1998. "Bright" aeolian dunes on Mars: Viking orbiter observations. LPSC XXIX [CDROM], Abstract # 1338.

Edgett, K.S., Christensen, P.R., 1994. Mars aeolian sand: regional variations among dark hued crater floor features. J. Geophys. Res. 99 (E1), 1997–2018.

Edgett, K.S., Malin, M.C., 2000. New views of Mars eolian activity, materials, and surface properties: three vignettes from the Mars Global Surveyor Orbiter camera. J. Geophys. Res. 105, 1623–1650.

Edgett, K.S., Geissler, P., Herkenhoff, K., 1992. Mars: The composition of dunes and other dark surficial material. LPSC XXIII [CDROM], Abstract # 327.

Feldman, W.C., Prettyman, T.H., Maurice, S., Plaut, J.J., Bish, D.L., Vaniman, D.T., Mellon, M.T., Metzger, A.E., Squyres, S.W., Karunatillake, S., Boynton, W.V., Elphic, R.C., Funsten, H.O., Lawrence, D.J., Tokar, R.L., 2004. The global distribution of near-surface hydrogen on Mars. J. Geophys. Res. 109 (E9). doi:10.1029/2003JE002160.

Fenton, L.K., Mellon, M.T., 2006. Thermal properties of sand from Thermal Emission Spectrometer (TES) and Thermal Emission Imaging System (THEMIS): spatial variations within the Proctor Crater dune field on Mars. J. Geophys. Res. 111 (E06). doi:10.1029/2004JE002363.

Fenton, L.K., Bandfield, J.L., Ward, A.W., 2003. Aeolian processes in proctor crater on Mars: sedimentary history as analyzed from multiple data sets. J. Geophys. Res. 108 (E12). doi:10.1029/JE002015.

Fryberger, S.G., Hesp, P., Hastings, K., 1992. Aeolian granule ripple deposits in Namibia. Sedimentology 39, 319–331.

Gay, S.P., 1962. Origen, distribucion y movimiento de las arenas eolicas en el area de Yauca a Palpa. Bol. Soc. Geol. Peru 37, 37–58.

Greeley, R., Iversen, J., 1985. Wind as a Geologic Process on Earth, Mars, Venus and Titan. Cambridge University Press, Cambridge.

Greeley, R., Lancaster, N., Lee, S., Thomas, P., 1992. Martian aeolian processes, sediments and features. In: Kieffer, H.H., Jakosky, B.M., Snyder, C.W., Matthews, M.S. (Eds.), Mars. University of Arizona Press, Tuscon.

Greeley, R., Skypeck, A., Pollack, J.B., 1993. Martian aeolian features and deposits: comparisons with general circulation model results. J. Geophys. Res. 98 (E2), 3183–3196.

Greeley, R., Squyres, S.W., Arvidson, R.E., 24 others, the Athena Science Team, 2004. Wind-related processes detected by the Spirit rover at Gusev crater, Mars. Science 305, 810–821.

Greeley, R., Arvidson, R.E., Barlett, 19 others, 2006. Gusev crater: wind-related features and processes observed by the Mars Exploration Rover Spirit. J. Geophys. Res. 111 (E02S09). doi:10.1029/2005JE002491.

Haberle, R.M., Murphy, J.R., Schaeffer, J., 2003. Orbital change experiments with a Mars general circulation model. Icarus 161, 66–89.

Head, J.W., Mustard, J.F., Kreslavsky, M.A., Milliken, R.E., Marchant, D.R., 2003. Recent ice ages on Mars. Nature 426, 797–802.

Hynek, B.M., Arvidson, R., Phillips, R.J., 2002. Geologic setting and origin of Terra Meridiani hematite deposit on Mars. J. Geophys. Res. 107 (E10). doi:10.1029/2002JE001891.

Jerolmack, D., Mohrig, D., Grotzinger, J., Fike, D., Watters, W.A., 2006. Spatial grain size sorting in eolian ripples and estimation of wind conditions on planetary surfaces: application to Meridiani Planum, Mars. J. Geophys. Res. 111 (E12S02). doi:10.1029/2005JE002544.
Kreslavsky, M.A., Head, J.W., 2000. Kilometer-scale roughness of Mars' surface: results from MOLA data analysis. J. Geophys. Res. 105, 26695–26712.
Kreslavsky, M.A., Head, J.W., 2002. Mars: nature and evolution of young latitude-dependent water-ice-rich mantle. J. Geophys. Res. 29 (15). doi:10.1029/2002GL015392.
Lancaster, N., 1995. Geomorphology of Desert Dunes. Routledge, London.
Lancaster, N., Greeley, R., 1987. Morphology of southern hemisphere intracrater dune fields, Reports of planetary geology and geophysics program — 1986. NASA TM89810, pp. 264–265 (abstract).
Langevin, Y., Poulet, F., Bibring, J.-P., Gondet, B., 2005. Sulphates in the northern region of Mars detected by OMEGA/Mars Express. Science 307, 1584–1586.
Laskar, J., Correia, A.C.M., Gastineau, M., Joutel, F., Levrard, B., Robutel, P., 2004. Long term evolution and chaotic diffusion of the insolation quantities of Mars. Icarus 170 (2), 343–364.
Malin, M.C., 1986. Rates of geomorphic modification in ice-free areas southern Victoria Land, Antarctica. Antar. J. U.S. 20 (5), 18–21.
Malin, M.C., Edgett, K.S., 2000. Science 288, 2330–2335.
Malin, M.C., Edgett, K.S., 2001. Mars Global Surveyor Mars Orbiter Camera: interplanetary cruise through primary mission. J. Geophys. Res. 106, 23,429–23,570.
Malin, M.C., Carr, M.H., Danielson, G.E., Davies, M.E., Hartmann, W.K., Ingersoll, A.P., James, P.B., Masursky, H., McEwen, A.S., Soderblom, L.A., Thomas, P., Veverka, J., Caplinger, M.A., Ravine, M.A., Soulanille, T.A., 1998. Early views of the Martian surface from the Mars Orbiter Camera of Mars Global Surveyor. Science 279, 1681–1685.
Malin, M.C., Edgett, K.S., Posiolova, L.V., McColley, S.M., Noe Dobrea, E.Z., 2006. Present day impact cratering rate and contemporary gully activity on Mars. Science 314, 1573–1577.
Mangold, N., 2003. Geomorphic evidence of lobate debris aprons on Mars at Mars Orbiter Camera scale: evidence for ice sublimation initiated by fractures. J. Geophys. Res. 108 (E4). doi:10.1029/2002JE1001885.
Mangold, N., 2005. High latitude patterned ground on Mars: classification, distribution and climatic control. Icarus 174, 336–359.
McCauley, J.F., Carr, J.R., Cutts, J.A., Hartmann, W.K., Masursky, H., Milton, D.J., Sharp, R.P., Wilhelms, D.E., 1972. Preliminary Mariner 9 report on the geology of Mars. Icarus 17, 289–327.
Melosh, H.J., 1989. Impact cratering, a geologic process. Oxford Monographs on Geology and Geophysics. Oxford University Press, New York.
Mustard, J.F., Cooper, C.D., Rifkin, M.K., 2001. Evidence for recent climate change from the identification of youthful, near-surface ice. Nature 412, 411–414.
Pierce, T.L., Crown, D.A., 2003. Morphologic and topographic analyses of debris aprons in the eastern Hellas region, Mars. Icarus 163, 46–65.
Presley, M.A., Arvidson, R., 1988. Nature and origin of materials exposed in the Oxia Palus -Western Arabia -Sinus` Meridiani Region, Mars. Icarus 75, 499–517.
Presley, M.A., Christensen, P., 1997a. Thermal conductivity measurements of particulate materials: 1. A review. J. Geophys. Res. 102 (E3), 6535–6549.
Presley, M.A., Christensen, P., 1997b. Thermal conductivity measurements of particulate materials: 2. Results. J. Geophys. Res. 102 (E3), 6551–6566.
Reiss, D., van Gasselt, S., Neukum, G., Jaumann, R., 2004. Absolute dune ages and implications for the time of formation of gullies in Nirgal Vallis, Mars. J. Geophys. Res. 109 (E06). doi:10.1029/2004JE002251.
Sharp, R.P., 1963. Wind ripples. J. Geol. 71, 617–636.
Squyres, S., Arvidson, R.E., Bell, J.F., 47 others, 2004. The Opportunity Rover's Athena Science investigation at Meridiani Planum, Mars. Science 306, 1698–1703.
Squyres, S., Arvidson, R.E., Bollen, D., 51 others, 2006. Overview of the opportunity Mars exploration rover mission to Meridiani Planum: eagle crater to purgatory ripple. J. Geophys. Res. 111 (E12S12). doi:10.1029/2006JE002771.
Sullivan, R., Thomas, P., Veverka, J., Malin, M.C., Edgett, K.S., 2001. Mass movement slope streaks imaged by the Mars Orbiter Camera. J. Geophys. Res. 106 (E10), 23,608–23,633.
Sullivan, R., Fike, D., Golombek, M.P., Greeley, R., Grotzinger, J., Jerolmack, D., Land, M.D., Malin, M.C., Soderblom, L.A., Squyres, S., Thompson, S.D., Watters, T.R., Whelley, P.L., 2004. Aeolian environments observed by the Mars Exploration Rovers (abstract). EOS Trans. AGU 85 (47) Jt. Assem. Suppl., Abstract P21B-04.
Sullivan, R., Banfield, D., Bell, J.F., Calvin, W., Fike, D., Golombek, M.P., Greeley, R., Grotzinger, J., Herkenhoff, K.E., Jerolmack, D., Malin, M.C., Ming, D., Soderblom, L.A., Squyres, S., Thompson, S.D., Watters, T.R., Weitz, C.M., Yen, A., 2005. Aeolian processes at the Mars Exploration Rover Meridiani Planum landing site. Nature 436, 58–61.
Sullivan, R., Arvidson, R., Grotzinger, J., Knoll, A., Golombek, M.P., Joliff, B., Squyres, S., Weitz, C.M., 2007. Aeolian geomorphology with MER Opportunity at Meridiani Planum, Mars. LPSC XXXVIII [CDROM], Abstract # 2048.
Thomas, P., 1981. North–south asymmetry of eolian features in Martian polar regions: analysis based on crater-related wind markers. Icarus 48, 76–90.
Thomas, P.C., Malin, M.C., Carr, M.H., Danielson, G.E., Davies, M.E., Hartmann, W.K., Ingersoll, A.P., James, P.B., McEwen, A.S., Soderblom, L.A., Veverka, J., 1999. Bright dunes on Mars. Nature 397, 592–594.
Thomas, M., Clarke, J.D., Pain, C.F., 2005. Weathering, erosion and landscape processes on Mars identified from recent rover imagery, and possible Earth analogues. Aust. J. Earth Sci. 52 (3), 365–378.
Tsoar, H., Greeley, R., Peterfreund, A.R., 1979. Mars: the north polar sand sea and related wind patterns. J. Geophys. Res. 84, 8167–8180.
Ungar, J., Haff, P.K., 1987. Steady state saltation in air. Sedimentology 34, 289–299.
White, B., 1979. Soil transport by winds on Mars. J. Geophys. Res. 84, 4643–4651.
Williams, K.K., Greeley, R., Zimbelman, J.R., 2003. Using overlapping MOC images to search for dune movement and to measure dune heights. LPSC XXXIV [CDROM], Abstract # 1639.
Williams, S.H., Zimbelman, J.R., Ward, A.W., 2002. Large ripples on Earth and Mars. LPSC XXXIII [CDROM], Abstract # 1508.
Wilson, I.G., 1972. Aeolian bedforms: their development and origins. Sedimentology 19, 173–210.
Wilson, S.A., Zimbelman, J.R., 2004. The latitude dependent nature and physical characteristics of transverse aeolian ridges on Mars. J. Geophys. Res. 109 (E10). doi:10.1029/2004JE002247.
Wilson, S.A., Zimbelman, J.R., Williams, S.H., 2003. Large aeolian ripples: Extrapolations from Earth to Mars. LPSC XXXIV [CDROM], Abstract # 1862.
Yizhaq, H., 2004. A simple model of aeolian megaripples. Physica A 338, 211–217.
Yizhaq, H., 2005. A mathematical model for aeolian megaripples on Mars. Physica A 357, 57–63.
Zimbelman, J.R., 1987. Spatial resolution and the geologic interpretation of martian morphology: implications for subsurface volatiles. Icarus 71, 257–267.
Zimbelman, J.R., 2000. Non-active dunes in the Archeron Fossae region of Mars between the Viking and Mars Global Surveyor eras. Geophys. Res. Lett. 27 (7), 1069–1072.
Zimbelman, J.R., 2003. Decameter-scale ripple-like features in Nirgal Vallis as revealed in THEMIS and MOC imaging data. Sixth international conference on Mars, abstract 3028.
Zimbelman, J.R., Wilson, S.A., 2002. Ripples and dunes in the Syrtis Major regions of Mars as revealed in MOC images. LPSC XXXIII [CDROM], Abstract # 1514.
Zimbelman, J.R., Williams, S.H., 2007. Dunes versus ripples: topographic profiling across terrestrial examples, with application to the interpretation of features on Mars. EOS Trans. AGU 88 (23) Jt. Assem. Suppl., Abstract P34A-07.
Zimbelman, J.R., Irwin, R.P., Williams, S.H., Bunch, F., Valdez, A., Stevens, S., 2007. Granule ripples on Earth and Mars: documented movement at Great Sand Dunes National Park, and implications for granule movement on Mars. LPSC XXVIII [CDROM], Abstract # 1324.
Zimbelman, J.R., Irwin, R.P., Williams, S.H., Bunch, F., Valdez, A., Stevens, S., in review. Documented granule ripple movement at Great Sand Dunes National Park and Preserve, with application to Mars, Geophys. Res. Lett.